BENTHIC FORAMINIFERAL ASSEMBLAGES FROM THE LAURENTIAN CHANNEL IN THE LOWER ESTUARY AND GULF OF ST. LAWRENCE, EASTERN CANADA: TRACERS OF BOTTOM-WATER HYPOXIA

Tiffany Audet[1],*, Anne de Vernal[1], Alfonso Mucci[2], Marit-Solveig Seidenkrantz[3], Claude Hillaire-Marcel[1], Vladislav Carnero-Bravo[4] and Yves Gélinas[5]

ABSTRACT

Over the past century, an increase in temperatures and a decrease in dissolved oxygen concentrations have been observed in the bottom waters of the Laurentian Channel (LC), throughout the Lower St. Lawrence Estuary (LSLE) and the Gulf of St. Lawrence (GSL), eastern Canada. To document the impact of these changes, we analyzed the benthic foraminiferal assemblages and geochemical signatures of four sediment cores taken in the LC. Radiometric measurements (^{210}Pb, ^{226}Ra, ^{137}Cs) indicate that the studied cores encompass the last 50 years of sedimentation in the LSLE and the last ~160 years in the GSL. The sedimentary record shows a 60 to 65% decrease in benthic foraminiferal taxonomic diversity in the LC since the 1960s. An accelerated change in the foraminiferal assemblages is observed at approximately the same time at all studied sites, around the late 1990s and the early 2000s, towards populations dominated by the hypoxia-tolerant indicator taxa *Brizalina subaenariensis*, *Eubuliminella exilis*, and *Globobulimina auriculata*. This evolution of assemblages reflects incursions of the hypoxic zone into the western GSL over the last decades. The results of our multivariate analyses highlight the potential of benthic foraminiferal assemblages as a proxy of bottom-water hypoxia.

INTRODUCTION

Historical measurements of dissolved oxygen (DO) concentrations in the bottom waters of the Lower St. Lawrence Estuary (LSLE) reveal a decrease of more than 50%, from ~125 μM L^{-1} in the 1930s to an average of ~60 ($\pm$6) μM L^{-1} between 1985 and 2018 (Gilbert et al., 2005; Jutras et al., 2020a). This impacted benthic marine ecosystems (Belley et al., 2010) with deleterious effects on the marine biota, including reduced growth and reproduction of commercially exploited marine species such as cod and northern shrimp (D'Amours, 1993; Chabot & Dutil, 1999; Dupont-Prinet et al., 2013). Furthermore, at hypoxic levels (<62.5 μM L^{-1}),

fish populations are increasingly vulnerable to additional stressors, natural and anthropogenic (Breitburg, 2002).

Oxygen depletion in the deep waters of the LSLE and the Gulf of St. Lawrence (GSL) has been attributed to various factors, including changes in the northwest Atlantic Ocean circulation pattern (Gilbert et al., 2005; Thibodeau et al., 2018; Jutras et al., 2020a), increased organic matter and nutrient fluxes (i.e., eutrophication) in the LSLE (Thibodeau et al., 2006, 2010; Jutras et al., 2020a, b), as well as increased bottom-water temperatures and the associated enhanced microbial respiration rates (Genovesi et al., 2011). In a recent study, Jutras et al. (2020a) determined that the dominant causes of oxygen depletion in the bottom waters of the Laurentian Channel (LC) may have changed over the last 50 years: the impact of enhanced microbial respiration in response to warmer bottom-water temperatures and eutrophication was likely determinant between the 1970s and the late 1990s, while a lower contribution of cold, oxygen-rich Labrador Current Water (LCW), relative to the warmer, oxygen-depleted North Atlantic Central Water (NACW) may be invoked between 2008 and 2018.

Regardless of the causes of oxygen depletion, the decrease in bottom-water oxygenation in the LC over the past century resulted in variations in the benthic foraminiferal assemblages preserved in the sediment (Thibodeau et al., 2006; Genovesi et al., 2011). As benthic foraminifera are sensitive to oxygenation (Sen Gupta & Machain-Castillo, 1993; Bernhard et al., 1997; Osterman, 2003; Platon et al., 2005), the abundance and diversity of species can be used to qualitatively and quantitatively (Ohkushi et al., 2013; Tetard et al., 2017, 2021a, b; Hoogakker et al., 2018; Erdem et al., 2020) assess the level of bottom-water DO concentrations. Temperature, primary production, organic carbon fluxes, and water mass distribution may also modulate the distribution of assemblages (e.g., Jorissen et al., 2007). Previous studies by Hooper (1975) and Rodrigues & Hooper (1982) provided a comprehensive overview of the benthic foraminiferal distribution in sediment collected in the LSLE and GSL in the 1970s. A few other studies documented recent changes in benthic foraminiferal assemblages at a few sites in the LSLE (Thibodeau et al., 2006, 2010) and GSL (Genovesi et al., 2011).

In this study, we analyzed the geochemical composition and micropaleontological content of four sediment cores collected in June 2018 in the LC of the LSLE and GSL. The records encompass decades to a few centuries. The two main objectives were: (1) to document how the recent and sub-recent benthic foraminiferal assemblages changed with the temporal and spatial evolution of the hypoxic zone across the LC, and (2) to semi-quantitatively evaluate the rates of changes in benthic foraminiferal assemblages in relation to bottom-water oxygenation.

[1] Département des Sciences de la Terre et de l'Atmosphère and Geotop-UQAM C.P. 8888, succ. Centre-ville, Montreal, Quebec, Canada H3C 3P8
[2] Department of Earth & Planetary Sciences and Geotop-McGill, 3450 University St., Montreal, Quebec, Canada H3A 0E8
[3] Department of Geoscience, Aarhus University, Høegh-Guldbergs Gade 2, 8000 Aarhus C, Denmark
[4] Instituto de Ecología, Universidad del Mar, Campus Puerto Ángel, Puerto Ángel, Oaxaca, México
[5] Geotop and Department of Chemistry & Biochemistry, Concordia University, 7141 Sherbrooke St. W. Montreal, Quebec, Canada H4B 1R6
* Corresponding author. E-mail: audet.tiffany@courrier.uqam.ca

STUDY AREA

The St. Lawrence Estuary system on the eastern coast of Canada is considered the largest semi-enclosed estuary in the world (Fig. 1). The freshwater discharge at Quebec City is estimated at 11,000 m^3 s^{-1}, second only to the Mississippi in North America (Bourgault & Koutinonsky, 1999). Its main bathymetric feature is the Laurentian Channel (LC), a 300–500 m deep, U-shaped submarine valley that extends ~1280 km landward from the continental shelf break to the head of the Lower St. Lawrence Estuary (LSLE) at Tadoussac (Figs. 1, 2). The LSLE and the Gulf of St. Lawrence (GSL) are characterized by estuarine circulation. During most of the sea ice-free season, the water column consists of a three-layer system based on its thermal stratification. The surface layer (0–30 m) flows seaward and results from the mixing of water from the northwest North Atlantic and freshwater from the St. Lawrence River and tributaries along its north shore (Dinauer & Mucci, 2018). It is characterized by relatively low salinities ($S_P = $ ~25–31, where S_P is the practical salinity) and seasonally variable temperatures. It overlies the Cold Intermediate Layer (CIL), a cold ($T = $ –1 to –2°C) and saline ($S_P = $ ~32 to 33) water mass that forms in winter in the gulf and flows landward at depths between 50 and ~150 m (Gilbert & Pettigrew, 1997; Galbraith, 2006). The deep waters below ~150 m originate from a mixture of warm, oxygen-poor North Atlantic Central Water (NACW) and cold, oxygen-rich Labrador Current Water (LCW), that enter the GSL through Cabot Strait (Dickie & Trites, 1983; Gilbert et al., 2005; Fig. 2B). They are relatively warm ($T = $ 4–7°C) and salty ($S_P = $ ~33–35). In winter, cooling and decreased freshwater input result in vertical mixing of the surface layer and CIL (Galbraith, 2006; Smith et al., 2006; Saucier et al., 2009). The surface waters are in contact with the atmosphere and, thus, well-oxygenated. However, the deep waters, which are isolated from the atmosphere by the persistent stratification, progressively lose DO through microbial respiration and remineralization of organic matter during their 4 to 7-year landward journey from the continental shelf break to the head of the LC (Bugden, 1991; Gilbert, 2004; Benoit et al., 2006). Consequently, highly oxygen-depleted bottom waters are observed throughout the LSLE and the western GSL (Gilbert et al., 2005; Jutras et al., 2020a, 2022). Any change in the ocean circulation that modifies the relative contributions of the LCW and NACW to the bottom waters of the LC, in addition to variations in organic matter fluxes and temperature, may play a role in modulating oxygenation conditions in the LSLE and GSL.

MATERIALS AND METHODS

CORING SITES AND SAMPLING

Four sediment cores were recovered in the LSLE and GSL in June 2018 aboard the *R/V Coriolis II* (Fig. 1; Table 1) using an Ocean Instrument Mark II box corer. Each box core (0.12 m^2 × 0.5 m high) was transferred to a specially designed stainless-steel glove box (Edenborn et al., 1987) for subsampling. Stations 23, 21, 18.5, and 16, at which the box cores were recovered, are part of a network of recurring stations along the LC that have been visited regularly over the

past 40 years. Each core was subsampled at 0.5-cm increments for the first centimeter. The core from station 23 was subsampled at 1-cm increments from 1 to 5 cm, 2-cm increments from 5 to 15 cm, and 3- or 4-cm increments to the bottom of the core. Cores from stations 21, 18.5, and 16 were subsampled at 1-cm increments to the bottom of the cores. At each depth interval, sediment samples were transferred and stored in two pre-weighed plastic vials. One set of vials was later weighed, freeze-dried, and weighed again to determine the water content. Sediment porosity was calculated from the water content, the salinity of the overlying seawater, and a dry sediment density of 2.65 g cm^{-3}. The freeze-dried sediments were then ground and homogenized with an agate pestle and mortar in preparation for later analyses (e.g., organic carbon). A known volume (6 to 8 mL) of a Rose Bengal solution (2 g L^{-1} in ethanol, density = 0.79 g mL^{-1}) was added to each of another set of vials to stain the living foraminifera. All subsamples we analyzed were stained, except for those below 25 cm from station 23. These vials were subsequently weighed, and the sediment porosity was used to determine the dry-sediment weight. The exact location, water depth, overlying water salinity, and DO concentration at each sampling station are reported in Table 1.

CORE CHRONOLOGY AND SEDIMENTATION RATES

The chronological framework was established from ^{210}Pb measurements for all studied cores, and from both ^{210}Pb and ^{137}Cs measurements for station 23. The ^{210}Pb activity in sediment was obtained indirectly by measuring the decay rate of its daughter isotope ^{210}Pb ($t_{1/2}$ = 138.4 days; α = 5.30 MeV) by alpha spectrometry assuming secular equilibrium. Following the protocol proposed by Flynn (1968), ^{209}Po was added to the freeze-dried samples as a spike to determine the extraction and counting efficiency and to measure the decay rate. The samples were submitted to a series of acid digestions (HCl, HNO_3, HF, and H_2O_2), and the purified polonium was deposited on a silver disk. The $^{209–210}$Po activities were measured in a silicon surface-barrier multichannel α-spectrometer (EGG-ORTEC, type 576A) coupled to a MAESTRO Multichannel Analyzer Emulation Software. Uncertainties were estimated from counting statistics to be approximately 6% for two standard deviations (2σ).

Sedimentation rates were estimated using the ^{210}Pb-decay constant (λ), the linear least-squares regression slope of the logarithmic function of excess ^{210}Pb and the CF (CRS) model with Monte Carlo uncertainty under the assumption of a constant rate of supply. The Plum software (Aquino-López et al., 2018) under R (R Core Team, 2021) was used to define the age models for each core (Fig. 3), taking into consideration the total (^{210}Pb$_{tot}$) and supported (^{210}Pb$_{sup}$) ^{210}Pb activities, the density (g cm^{-3}) of samples, and the coring date.

The supported fraction of ^{210}Pb was determined in the bottom section of the cores using the activity of the parent isotope ^{226}Ra. To confirm the validity of the chronological framework, we measured the vertical distribution of ^{137}Cs activity in the sediment core recovered from station 23. The ^{137}Cs activity was measured at 661.6 keV and the ^{226}Ra activity was measured at 295.22, 352, and 609.32 keV using a Canberra low-background high-purity Ge well-detector.
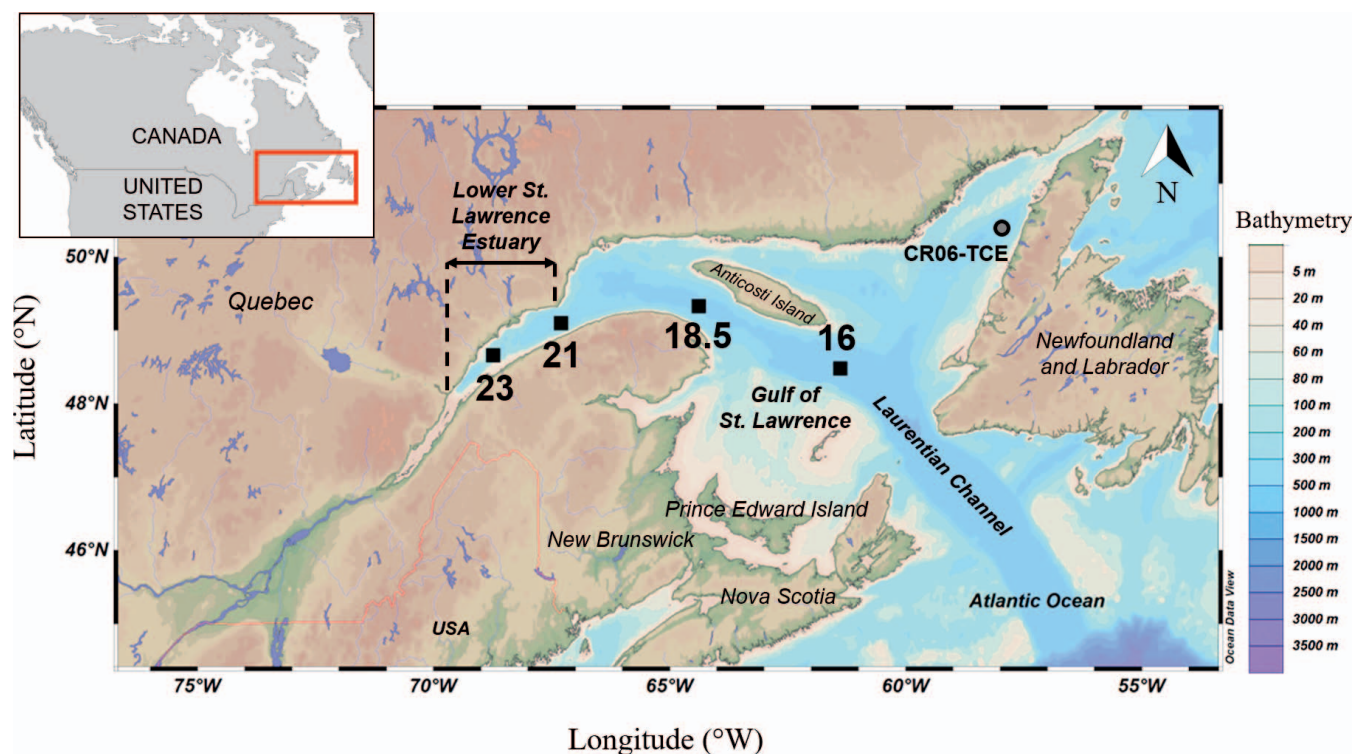
FIGURE 1. Map of the St. Lawrence Estuary and Gulf with location of the study sites (23, 21, 18.5 and 16) in the LC (see Table 1 for precise location and bottom-water properties), as well as core CR06-TCE in the Esquiman Channel (Thibodeau et al., 2013). The cores were collected in 2018; sediment cores recovered at station 23 in 2000 and station 16 in 2005 were respectively analyzed and interpreted by Thibodeau et al. (2006) and Genovesi et al. (2011).

The reproducibility of ^{226}Ra and ^{137}Cs activity measurements was estimated at ±1% (1σ) based on replicate analyses ($n = 6$) of the Columbia River Basalt reference material (BCR-2; USGS).

SEDIMENTARY CARBON AND NITROGEN ANALYSES

Total carbon (C_{tot}) and total nitrogen (N_{tot}) content of the freeze-dried, ground, and homogenized sediment samples were determined using a Carlo Erba™ NC 2500 elemental analyzer (NC2500TM) at the Geotop Research Center. The inorganic carbon (IC) content of the sediments was determined independently using a UIC coulometer, following acidification of a weighed aliquot of the freeze-dried samples and CO_2 extraction. The precision of this analysis is better than ±2%. The organic carbon content (C_{org}) was obtained from the difference between total carbon (C_{tot}) and inorganic carbon (IC):

$$C_{org} = C_{tot} - IC$$

The standard deviation (1σ) on the C_{tot} and N_{tot} analyses was estimated at, respectively, 0.1% and 0.3%, based on replicate measurements of organic analytical standard substances (acetanilide, atropine, cyclohexanone-2,4-dinitrophenyl-hydrazone, and urea).

For isotopic analyses of C_{org}, freeze-dried, ground and homogenized sediment samples were fumed in a desiccator for 48 hours in the presence of concentrated hydrochloric acid to dissolve carbonate phases. The isotopic composition of C_{org} ($\delta^{13}C_{org}$) was measured with a Micromass Isoprime™ ratio mass spectrometer in-line with an Elementar Vario MicroCube™ elemental analyzer in continuous flow mode. Data are reported in the δ notation in ‰ with respect to

TABLE 1. Location of the core sites and bottom-water properties (practical salinity and dissolved oxygen, DO) measured during sampling.

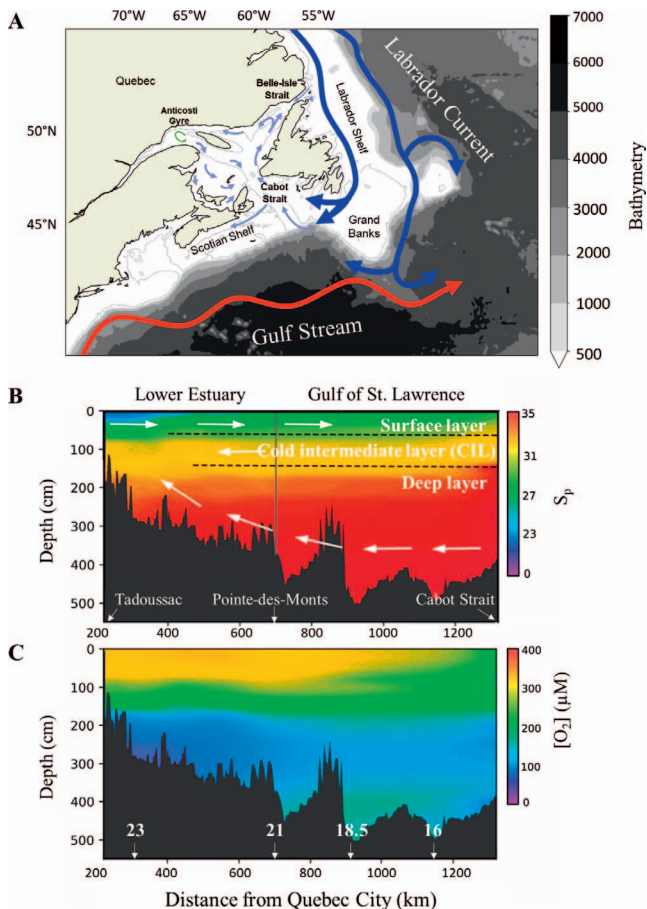| Station	Latitude (N)	Longitude (W)	Water depth (m)	Bottom-water practical salinity	Bottom-water dissolved oxygen concentration (μM)	Core length (cm)	Analyzed core length (cm)
23	48°40.15'	−68°44.25'	340	34.52	56.2	41	41
21	49°05.00'	−67°18.15'	325	34.46	58.2	20	13
18.5	49°19.50'	−64°23.30'	389	34.78	77.0	20	15
16	48°29.80'	−61°24.70'	418	34.93	117.0	20	20

FIGURE 2. **A** Map of the main currents of the LSLE and GSL. The arrows represent the approximate position of: the LCW in dark blue; the Gulf Stream in red; the Anticosti Gyre in green; the inner currents of the Gulf in light blue. **B** Schematic representation of the summer three-layer stratification along the LC. Colors represent practical salinity. **C** Dissolved oxygen (DO) concentrations and approximate locations of stations 23, 21, 18.5, and 16 along the LC. Data extracted in 2020 from the BioChem database made available by the Department of Fisheries and Oceans Canada. Modified after Jutras et al. (2020b).

V-PDB (Coplen, 1995; Fig. 4). As determined from replicate measurements of standard materials, the analytical uncertainty was estimated at ±0.1‰. To normalize the results on the NBS19-LSVEC scale, two internal reference materials ($\delta^{13}C = -28.73 \pm 0.06$‰ and $\delta^{13}C = -11.85 \pm 0.04$‰) were used, and a third reference material ($\delta^{13}C = -17.04 \pm 0.11$‰) was analyzed as an unknown to assess the accuracy of the normalization.

BENTHIC FORAMINIFERAL ANALYSES

Each sediment sample was treated according to the procedure described by de Vernal et al. (1999). Depending on the liquid content of the subsamples, 5 to 13 cm³ of wet sediment were weighed, dried at room temperature, weighed again, and wet-sieved through 63 μm and 106 μm mesh sieves. Both these fractions were examined under a binocular microscope at 40× and 100× magnification. Calcareous and agglutinated benthic foraminifera were hand-sorted, enumerated, identified, and counted according to the nomen-

clature of Rodrigues (1980) and Loeblich & Tappan (1987). Planktonic foraminifera were not counted, as they only occurred occasionally. Well-preserved specimens of calcareous benthic foraminifera, photographed using a Keyence™ microscope, are presented in Figures A1 and A2. The list of all observed taxa and their relative abundance (e.g., rare, occasional, common) in the LSLE and GSL sediments are reported in Table A1.

In oxygen-depleted environments, the protoplasm of dead foraminifera may be preserved for several months (Bernhard, 1988; Corliss & Emerson, 1990), which could lead to an overestimation of the abundance of living individuals from Rose Bengal staining (Fontanier et al., 2002). Hence, we applied strict staining criteria, as described in Fontanier et al. (2002), to overcome the inaccuracies of the method, by counting individuals as living only if the Rose Bengal stained all chambers except the last one. Partly stained tests were still noted as an indicator of the presence of an undecayed protoplasm.

The relative abundance of various taxa, expressed as percentages, were calculated for all taxa but only common and occasional taxa are reported. The relative abundance of taxa that accounts for ≥3% of the assemblages in at least one sample per core are presented in Figure 5.

Multivariate analyses using the CANOCO 5 software (ter Braak & Šmilauer, 2012) were conducted with the percentages of calcareous taxa to help define zonation and assemblages. We performed principal component analyses (PCA) and illustrated the scores of the two main principal components (first axis PC1; and second axis, PC2) on ordination diagrams available in the Supplementary Materials. We also performed a constrained redundancy analysis (RDA) based on the calcareous assemblage at station 23 and temperature and DO as environmental variables. Finally, we calculated dissimilarity coefficients using the squared chord distance (SCD) to define the depth of the most pronounced changes in assemblages (Overpeck et al., 1985). The PCA, RDA, and multivariate SCD analyses were conducted on taxa that account for ≥3% of the assemblage in at least one sample to reduce crowding and the effect of rare taxa on the analyses.

RESULTS AND DISCUSSION

EXCESS ²¹⁰PB, ¹³⁷CS ACTIVITIES AND SEDIMENTATION RATES

Uniform values of the excess ^{210}Pb activity (^{210}Pb$_{ex}$) in the upper part of the cores are interpreted as delimiting the depth of the mixed layer (Fig. 3). At station 23, the $\ln(^{210}\text{Pb}_{ex})$ data can be fit to a simple linear equation with a slope of -0.05 ($R^2 = 0.98$), corresponding to a sedimentation rate of ~0.70 ± 0.03 cm a^{-1}. At station 21, the linear fit to the $\ln(^{210}\text{Pb}_{ex})$ data yields a slope of -0.08 ($R^2 = 0.96$), corresponding to a sedimentation rate of ~0.42 ± 0.03 cm a^{-1} (Fig. 3B). At station 18.5, the linear fit to the $\ln(^{210}\text{Pb}_{ex})$ data yields a slope of -0.12 ($R^2 = 0.96$), corresponding to a sedimentation rate of ~0.27 ± 0.03 cm a^{-1} (Fig. 3C). At station 16, the results suggest that there may have been a change in sedimentation rates. The first slope over the upper 5 cm is -0.10 ($R^2 = 0.96$), corresponding to a sedimentation rate of ~0.31 ± 0.03 cm a^{-1}. The second slope over the 5−20 cm interval is -0.04 ($R^2 = 0.97$), corresponding to a sedimenta-
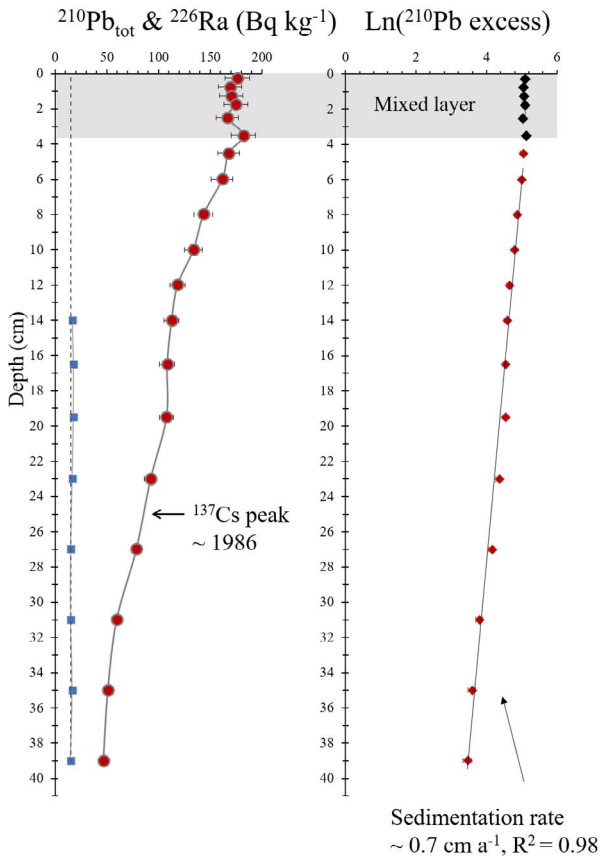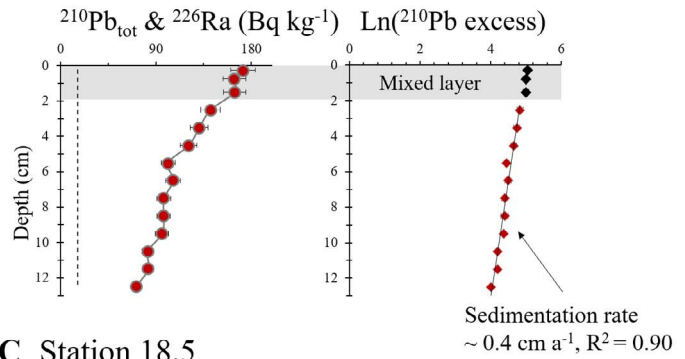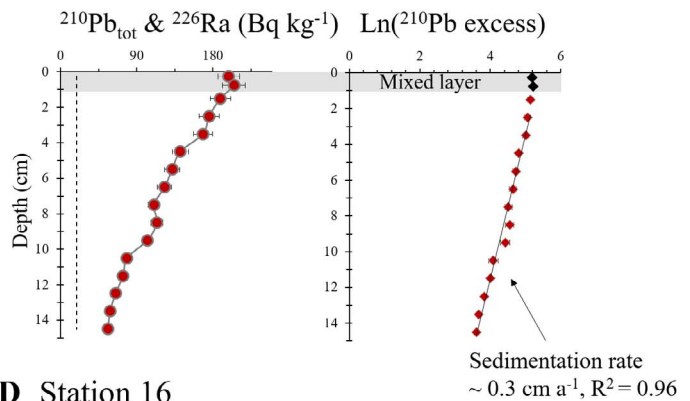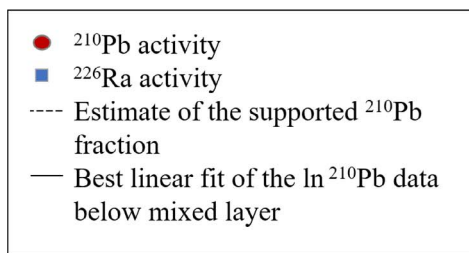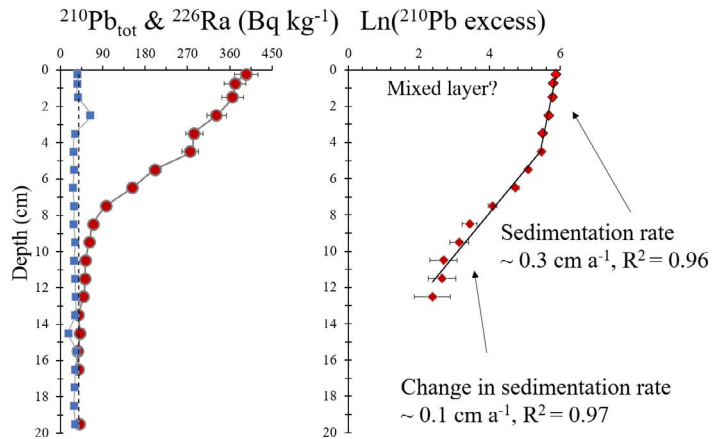
FIGURE 3. Excess ^{210}Pb (ln) at **A** station 23 **B** station 21 **C** station 18.5 and **D** station 16. The circles represent the ^{210}Pb data. The squares represent the ^{226}Ra data from which the supported ^{210}Pb value (vertical dotted line) was estimated. At stations 21 and 18.5, the supported ^{210}Pb was estimated from data at the bottom section of the cores. The depth of the mixed layer (highlighted in grey) and/or sediment density change is not taken into consideration in the sedimentation rate calculation. Sedimentation rates were calculated from the linear regression below the mixed layer.

tion rate of ~0.11 ± 0.03 cm a^{-1} (Fig. 3D). Based on ^{210}Pb and ^{137}Cs measurements, Genovesi et al. (2011) also concluded that sedimentation rates in this area of the GSL may have varied through time over the previous two centuries. The sedimentation rates obtained in this study are consistent with estimates from Thibodeau et al. (2006) at station 23 and Genovesi et al. (2011) near station 16.

Since none of the ^{210}Pb$_{ex}$ profiles follow a decreasing exponential curve under the mixed layers, we assume a constant flux of ^{210}Pb to set a chronology. Our chronological framework established with the Plum model was confirmed by measurements of ^{137}Cs activities throughout the core recovered at station 23. Assuming the location of the ^{137}Cs peak at a sub-bottom depth of ~25 cm (not shown) corresponds to 1986 CE, the year of the Chernobyl incident, our ^{210}Pb-based age model at this station is accurate. Furthermore, the correlation of the benthic foraminiferal species *Brizalina subaenariensis* and *Eubuliminella exilis* between our station 23 core and core CR02-23 investigated by Thibodeau et al. (2006), taken at the same location, indicates that the bottom of our core (41 cm) is not older than ~1960, as the two species first appeared around this time in CR020-23.
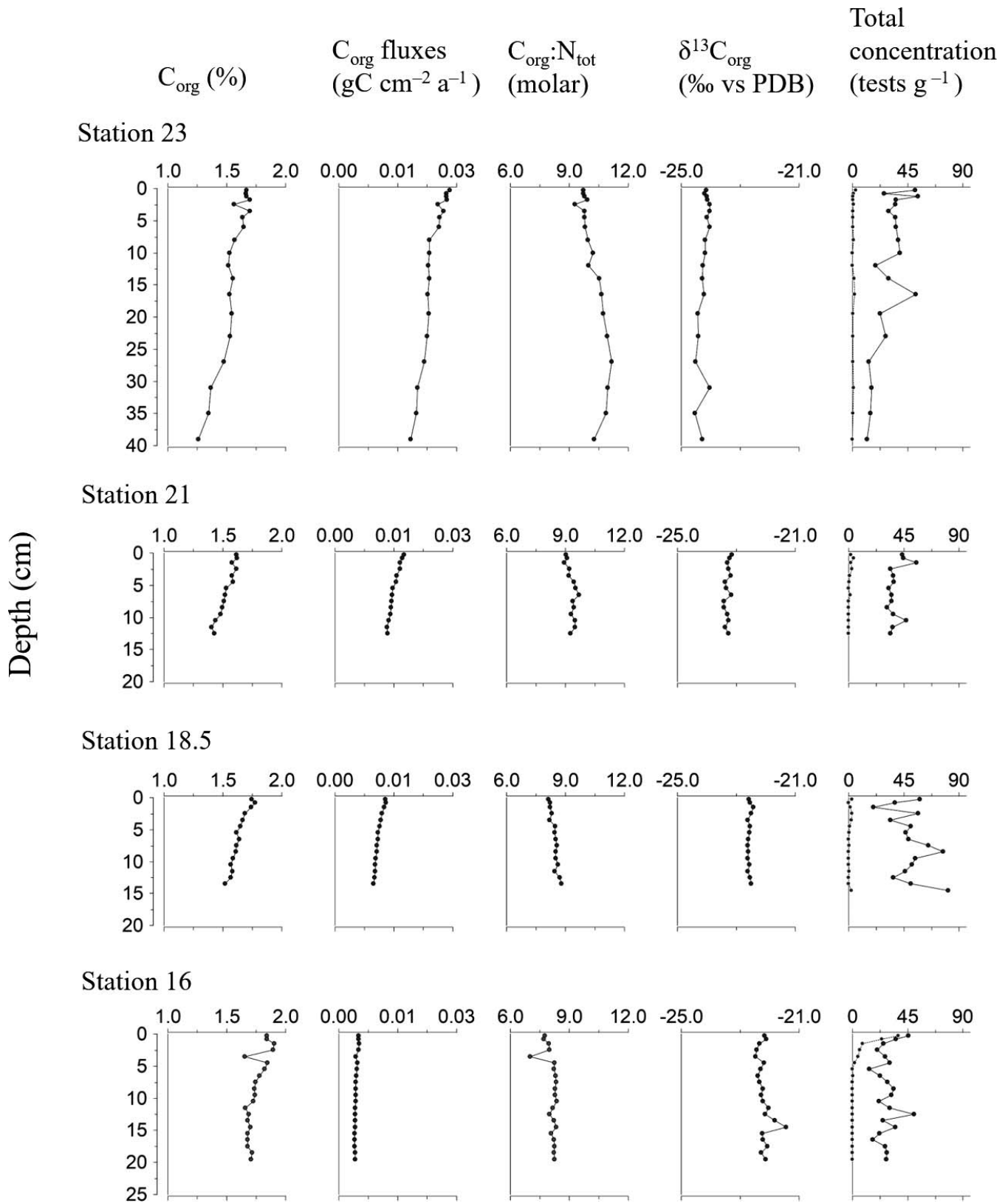
FIGURE 4.   Organic carbon (C_{org}), C_{org} fluxes, ratio of organic carbon to total nitrogen (C_{org}:N_{tot}), $\delta^{13}C_{org}$, and total foraminiferal test concentrations (dashed lines for agglutinated), as a function of depth, at stations 23, 21, 18.5, and 16.
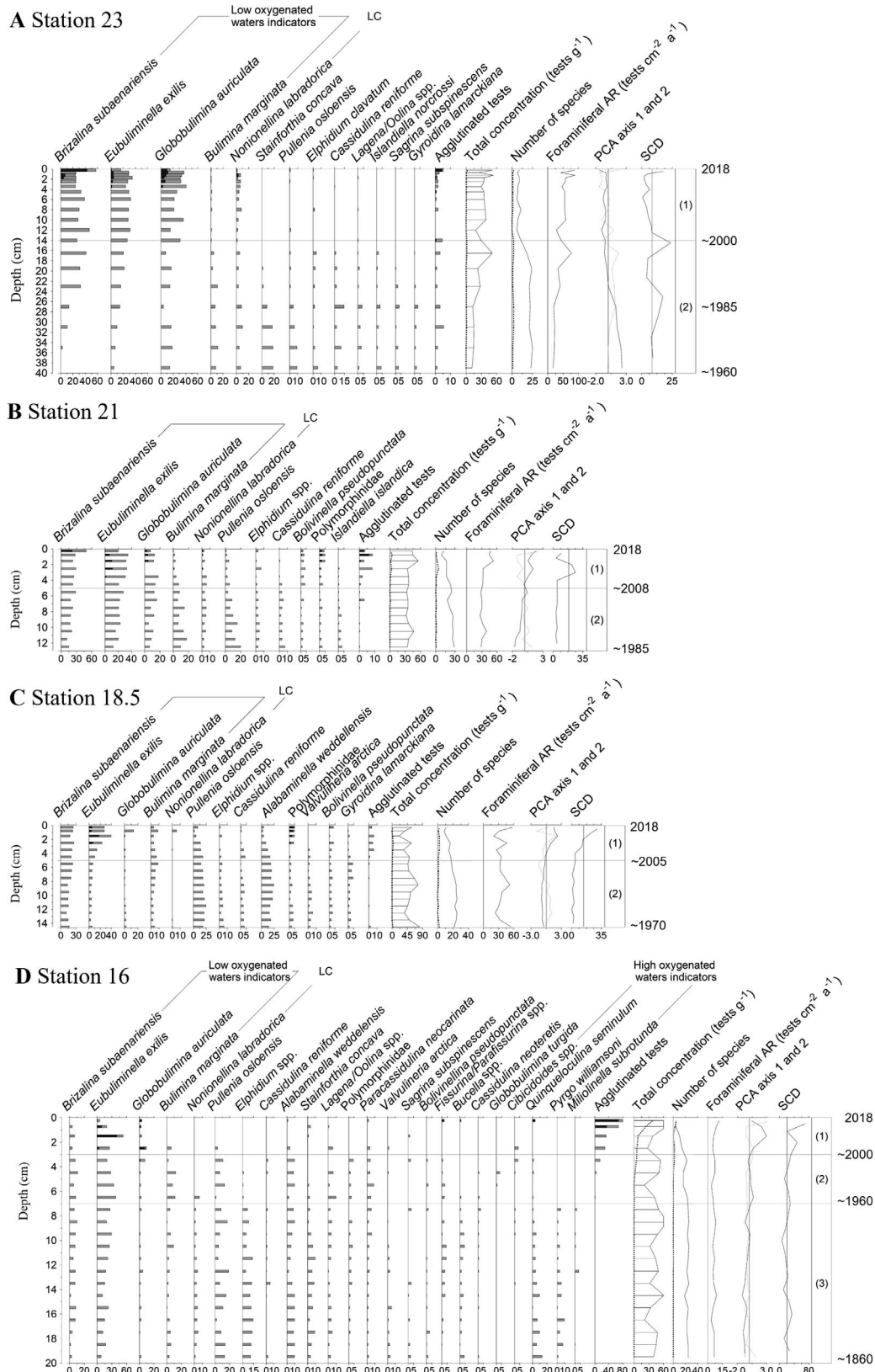
FIGURE 5. Calcareous benthic foraminiferal assemblages from **A** station 23 **B** station 21 **C** station 18.5 and **D** station 16. Percentages of the main taxa ($\geq$3% in at least one sample), total concentration (tests g^{-1}), number of species, accumulation rates (tests cm^{-2} a^{-1}), PCA scores, and SCD coefficient, as a function of depth. The black portion of the histograms indicates the percentage of stained (living) specimens. The dotted lines in the total concentration and number of species diagrams correspond to the agglutinated tests. The PC1 score is given by the black solid line and the PC2 score is presented by the grey dashed line. Horizontal grey lines and numbers in brackets indicate zones defined by PCA scores explained in the text.

According to our age models and the above-mentioned correlation, we can assess that the cores we recovered from station 23 encompass the last ~50 years of sedimentation (i.e., ~1965–2018 CE). Thus, the geochemical and micropaleontological analyses performed at 0.5- and 1-cm intervals provide time series with sub-annual to decadal resolution. The Plum settings and output for each station are available in the Supplementary Materials (Fig. S1).

GEOCHEMISTRY OF SEDIMENTARY ORGANIC MATTER

The organic carbon content of the sediment in the four study cores ranges from 1.26% to 1.91%. There is a slight increase in organic carbon content from the LSLE to the GSL, with an average of 1.55% at station 23, 1.53% at station 21, 1.61% at station 18.5, and 1.75% at station 16. However, these values do not necessarily translate into higher organic carbon fluxes and productivity as they may reflect a lower dilution by organic material inputs of terrestrial origin, as would suggest the $\delta^{13}C_{org}$ data. The organic carbon fluxes can be computed based on the estimated sedimentation rates (Fig. 4). The average total mass accumulation rates are 1.54, 0.99, 0.68, and 0.25 g cm^{-2} a^{-1} at stations 23, 21, 18.5, and 16, respectively.

The organic carbon content of all four cores typically decreases slightly with depth, while the C_{org}:N_{tot} molar ratio increases slightly (Fig. 4). This may be attributed to the preferential degradation of nitrogen-rich organic matter during early diagenesis (Meyers, 1997; Muzuka & Hillaire-Marcel, 1999).

The $\delta^{13}C_{org}$ data show distinct signatures at each study site, with lower values in the LSLE and higher values in the GSL. The mean $\delta^{13}C_{org}$ are –24.2‰ at station 23, –23.2‰ at station 21, –22.6‰ at station 18.5, and –22.1‰ at station 16. They reflect the higher proportions of terrestrial versus marine organic matter at stations in the LSLE than in the GSL.

COMPOSITION OF ASSEMBLAGES AND SPECIES DIVERSITY

Specimens of calcareous and agglutinated taxa were well preserved, with few broken or altered tests. A total of 52 calcareous and four agglutinated taxa were identified in the >63 μm fraction of the four study cores. Among those, seven calcareous taxa are common to abundant at all sites, representing >10% of the assemblages in many samples: *Brizalina subaenariensis*, *Eubuliminella exilis*, *Globobulimina auriculata*, *Bulimina marginata*, *Nonionellina labradorica*, *Pullenia osloensis*, and *Elphidium clavatum*. Additionally, nearly 25 taxa are considered occasional, whereas 20 taxa are considered rare as they account for <3% of the assemblages in samples of each core.

We observed a loss in the number of species towards the core top at all stations, indicating a loss of diversity over time (Fig. 5). In the LSLE, at station 23, the number of species decreased by about 60% since the 1960s. In the GSL, at station 16, species diversity dropped by almost 65% over the same time period, while the entire sedimentary record shows a decrease of 75% over the last ~160 years. The number of species decreased by about 50% over the last ~30 years

at station 21, and by about 60% over the last ~50 years at station 18.5.

In the LSLE, the overall assemblage is dominated by the calcareous taxa *B. subaenariensis*, *E. exilis*, *G. auriculata*, *B. marginata*, *N. labradorica*, and *P. osloensis* (Fig. 5A, B), which together account for about 80% of the assemblages in cores from stations 23 and 21. Important secondary taxa in the LSLE include *Cassidulina reniforme* and *E. clavatum*.

In the GSL, we observe a higher diversity than in the LSLE with assemblages dominated by *B. subaenariensis*, *E. exilis*, *P. osloensis*, and *Alabaminella weddellensis* which together account for ~67% of the assemblage at station 18.5. At station 16, they are dominated by *E. exilis* and *P. osloensis*, which account for ~40% of the assemblage. Secondary species include *C. reniforme*, *Elphidium* spp. (mostly *E. clavatum*), *G. auriculata*, *B. marginata*, and *N. labradorica*.

Brizalina subaenariensis is the dominant species in all study cores, except at station 16 where *E. exilis* dominates. This suggests that *B. subaenariensis* has a higher tolerance for reduced oxygen levels than *E. exilis*, since the bottom-water DO concentration is much higher (~117 μM) at station 16 than at sites in the western part of the LC (<80 μM; Fig. 6).

MULTIVARIATE ANALYSES

Foraminiferal Zonation of the Sedimentary Environmental Records

The PCA results from each core analyzed independently show different ordinations, but the opposition between *B. subaenariensis* and *E. exilis* versus most other taxa remains a characteristic feature (see Supplementary Materials, Fig. S2). Three main assemblage zones were defined based on these PCA results, and their boundaries were set using both PC1 and PC2, and maximum SCD coefficients (Fig. 5).

Zone 1 is generally characterized by the dominance of *B. subaenariensis*, *E. exilis*, *G. auriculata*, which are low-oxygen tolerant species (Kaiho, 1994; Sen Gupta, 1999; Brüchert et al., 2000), as well as by a low diversity of species. It encompasses approximately the last 20 years, from the early 2000s to 2018, as derived from the age model in the core from station 23.

Zone 2 is likely a transitional zone, as it corresponds to a decrease in species diversity and the successive decrease or disappearance of most occasional taxa, such as *B. marginata*, *P. osloensis*, *E. clavatum*, as well as an increased abundance of *B. subaenariensis*, *E. exilis*, and *G. auriculata*. It encompasses a period from about ~1960 to ~2000 in stations 23 and 16.

Zone 3 is observed in the lower part of the core from station 16. It is characterized by the highest taxonomical diversity, low percentages of *B. subaenariensis* and *G. auriculata*, and the common occurrence of *E. exilis*, *P. osloensis*, and *E. clavatum*, as well as the indicator of well-oxygenated waters *Quinqueloculina seminulum* (Kaiho, 1994).

The significant loss in species diversity and the change towards assemblages dominated by low oxygen-tolerant taxa between Zone 1 and 2 around the late 1990s and early 2000s in all four cores illustrate how rapidly benthic foraminifera responded to the changes in ocean circulation happening at the same time (Jutras et al., 2020a).
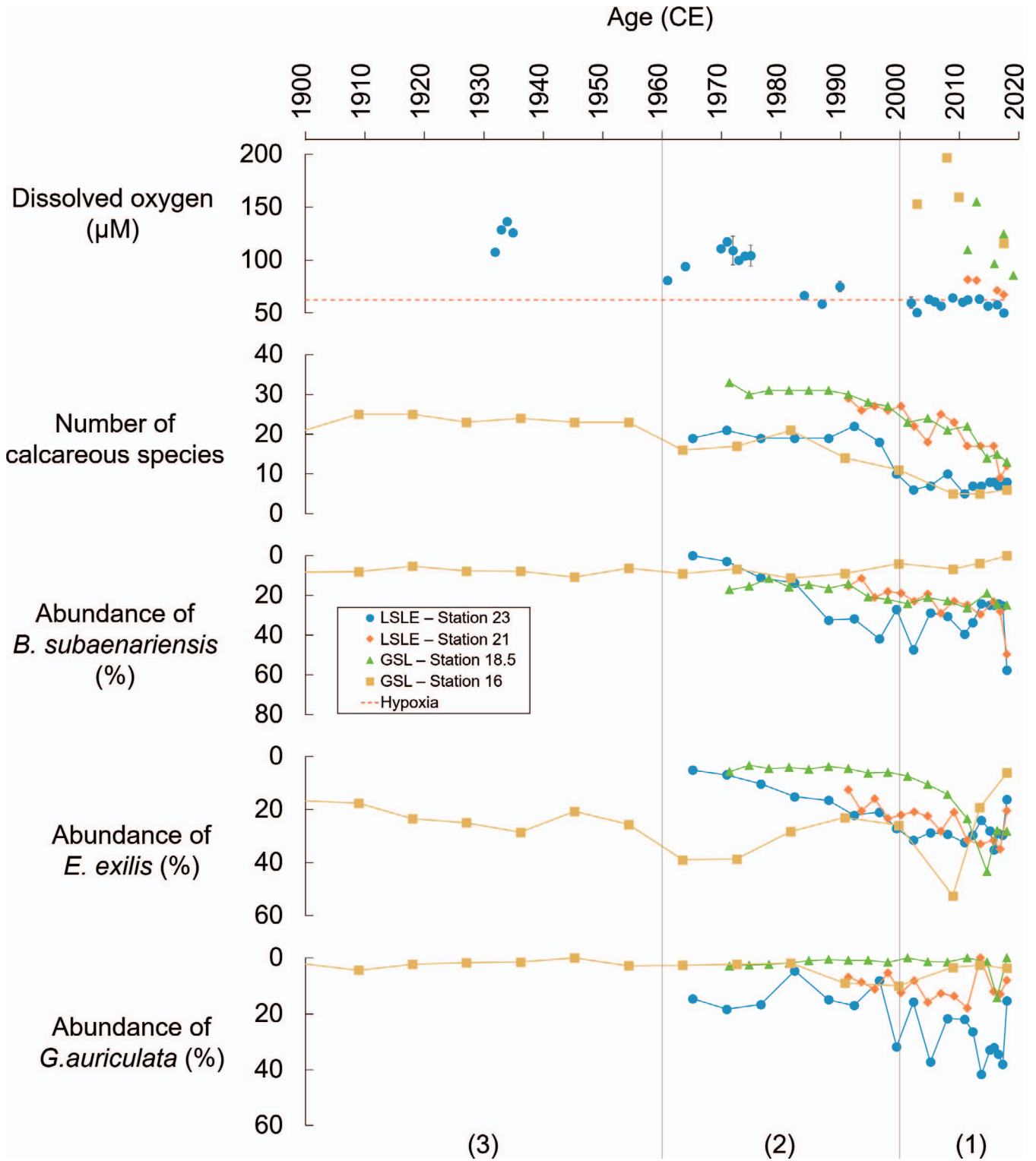
FIGURE 6. Record of dissolved oxygen (DO) concentrations at 250 to 355 m of water depth in the LSLE based on data extracted from the BioChem database made available by the Department of Fisheries and Oceans Canada, and a compilation of data acquired on the *R/V Coriolis II* (extended from Gilbert et al., 2005; Jutras et al., 2020a, see Table S2). The number of calcareous species, and percentages of *B. subaenariensis*, *E. exilis*, and *G. auriculata*. The dotted line indicates the severe hypoxia threshold (<62.5 µM). Vertical grey lines and numbers in brackets indicate zones defined by PCA scores and correspond to the zones described in Figure 5.

Benthic Foraminifera and Environmental Conditions in the LSLE and GSL

The data from station 23, where instrumental measurements of bottom-water conditions are available for an extended period of time (~90 years), allowed us to perform an RDA to further evaluate the relationship between bottom-water temperatures, DO concentrations, and the downcore measurements of geochemical variables with benthic foraminiferal assemblages (ordination diagram available in the Supplementary Materials; Fig. S3; Table S1). The RDA reveals that oxygenation is the principal environmental parameter affecting the calcareous benthic foraminiferal assemblages in our study area, as it is highly correlated with the RDA axis 1 ($R^2 = 0.9024$), which explains 52% of the variance. The relationship with food quality, as illustrated by the $C_{org}:N_{tot}$ and $\delta^{13}C_{org}$, also stands out as an important environmental parameter, as suggested by the RDA axis 2 ($R^2 = 0.4225$ and $R^2 = 0.3984$, respectively), which explains 11% of the variance.

With the DO concentrations highlighted as the principal environmental parameter affecting benthic foraminifera, the results of the PCA in all analyzed samples (see Fig. 7) combined with ecological notes from the literature led us to define three main groups of benthic foraminifera in relation to the oxygenation conditions of their habitat. Ordination diagram shows that PC1, which represents 47% of the variance, is weighted by a strong opposition between *B. subaenariensis*, *E. exilis*, and *G. auriculata* on the positive side and all other species on the other site.

The first group, characterized by the three co-dominant species *B. subaenariensis*, *E. exilis*, and *G. auriculata*, is related to hypoxic bottom-water conditions ($[DO] \leq 62.5\ \mu M$) in the LC. This assemblage is typically associated with Zone 1 assemblages at stations in the LSLE. At stations in the GSL, *G. auriculata* is not a co-dominant species.

The second group is characterized by the presence of *Islandiella islandica*, *A. weddellensis*, *Gyroidina lamarckiana*, *P. osloensis*, and *Bolivinellina pseudopunctata*. It corresponds to varying, but on average relatively low bottom-water DO concentrations. Based on the assemblages observed in the core from station 23, we estimate that bottom-water DO concentrations ranged between 62.5 and ~100 μM.

The third group is characterized by the presence of *Paracassidulina neocarinata*, *Buccella* spp., *Lagena/Oolina* spp., *Q. seminulum*, *Pyrgo williamsoni*, *Stainforthia concava*, and *Elphidium* spp. It would be an indicator of relatively high bottom-water oxygen levels in the LC. Given the assemblages in the core from station 23, we estimate that bottom-water DO concentrations ranged from ~100 to ~140 μM when this assemblage was present at the sediment surface.

It should be noted that these groups are specific to the LC, LSLE, and GSL, and these proxies may not be applicable to the global ocean. Furthermore, the benthic environmental conditions defined by these groups are likely to have changed through time. Although bottom-water oxygenation conditions in the LSLE have been low over the past 40 years, there may have been episodic pulses of higher oxygen concentrations, as suggested by the variability of the areal extent of the hypoxic zone (Jutras et al., 2022) and the co-

occurrence of both high and low oxygen-tolerant species in groups 2 and 3.

CHANGES IN BOTTOM-WATER CONDITIONS

Mix of Water Masses Leads to Complex Benthic Foraminiferal Assemblages

The foraminiferal assemblages of the LSLE and the GSL include a number of species that are today found in Arctic and subarctic environments (e.g., *C. reniforme*, *I. islandica*, *Islandiella norcrossi*, *N. labradorica*, *S. concava*, *Valvulineria arctica*; Osterman et al., 1999; Lloyd et al., 2007; Jennings et al., 2020; Cage et al., 2021; Ovsepyan et al., 2021). However, we also identified species that are today abundant in temperate to subtropical regions. Noteworthy are *Sagrina subspinescens* (commonly named *Bolivina subspinescens*), a relatively warm Atlantic Water species (Rasmussen & Thomsen, 2004), and *P. neocarinata*, a species found along the western Atlantic margin from the Gulf of Mexico to the coast of Nova Scotia (Cushman, 1922; Phleger & Parker, 1951; all as *C. laevigata* var. *carinata* Cushman; Parker, 1954; Vilks & Rashid, 1976: as *C. laevigata*; Sen Gupta & Aharon, 1994; Platon, 2001; Cage et al., 2021). Moreover, many of the species we observe are known to tolerate low bottom-water oxygenation (*B. subaenariensis*, *E. exilis*, *G. auriculata*, and *B. marginata*), including *P. neocarinata* that has also been reported to tolerate the hypoxic conditions that develop seasonally in the Gulf of Mexico (Tichenor, 2013). This complex combination of species may be explained by inputs from three different water masses into the GSL (Fig. 2): the LCW that brings oxygen-rich polar water, the NACW that supplies oxygen-poor warm water, and freshwater from St. Lawrence River that brings nutrients from a large watershed.

Benthic Foraminiferal Response to Changes in Bottom-water Conditions in the LC

In response to the recent changes in the ocean circulation in the northwestern Atlantic Ocean, the consequent modification of benthic environmental conditions in the GSL (Genovesi et al., 2011; Thibodeau et al., 2018; Jutras et al., 2020a), and the development of hypoxic waters (Jutras et al., 2022), benthic foraminiferal assemblages swiftly shifted towards the quasi-exclusive dominance of low-oxygen tolerant or indicator species (i.e., *B. subaenariensis*, *E. exilis*, and *G. auriculata*; Figs. 6, 8) at the expense of the other taxa (Fig. 5). At station 23, where hypoxic conditions (<62.5 μM) have been persistent for nearly 40 years, these three taxa make up 90% of the calcareous assemblage. Although the geographical expansion of the hypoxic zone had only made occasional incursions into the western GSL until 2020 (Jutras et al., 2022), these incursions are reflected in the important decrease of species diversity throughout the LC.

At stations 18.5 and 16 in the GSL, the lack of a long-term instrumental record of DO prevents defining quantitative relationships with foraminiferal assemblages and the relative abundances of *B. subaenariensis* and *E. exilis*. Both species are present from the base of the study cores dating back to ~1860s and their abundance varies little throughout the cores, especially at station 16 (Fig. 5D). The proliferation of *E. exilis* at station 16 seems to be fostered by temperature,
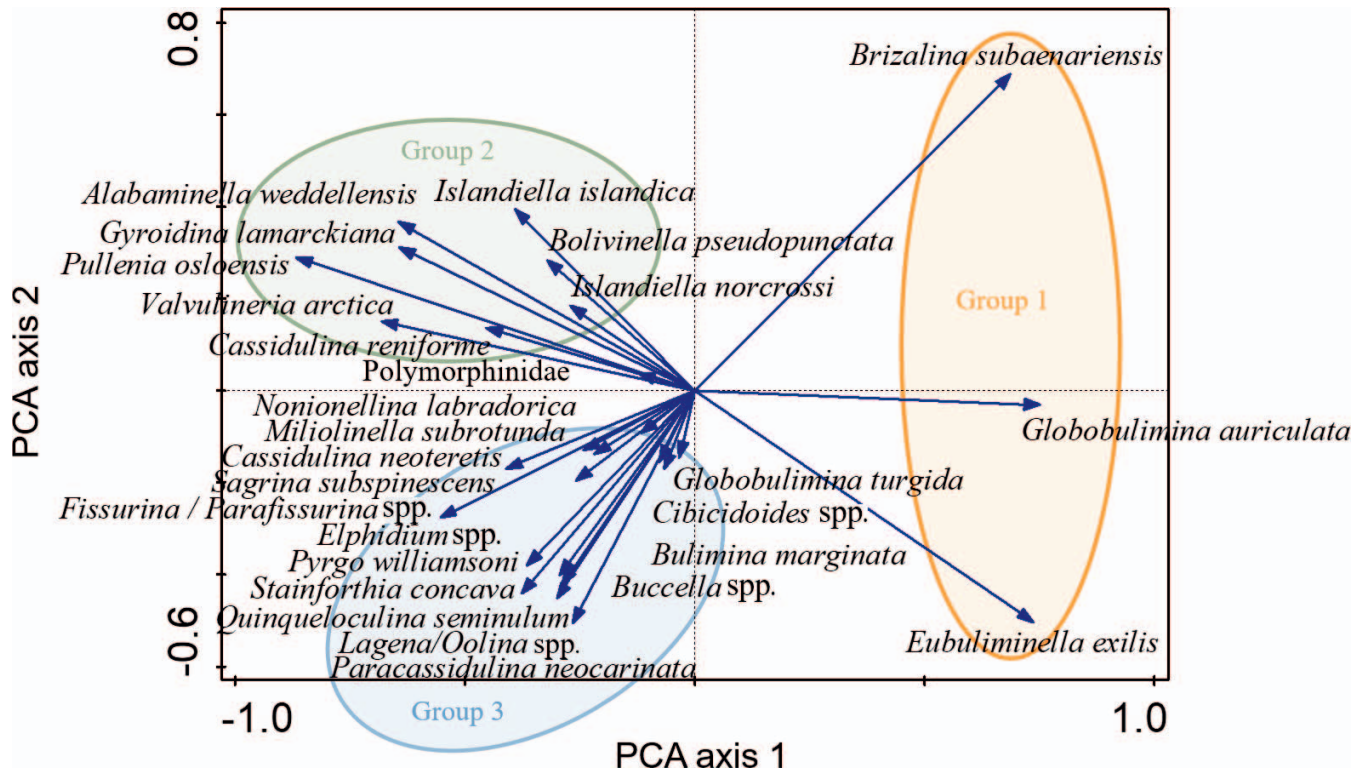
FIGURE 7. Ordination diagram of calcareous benthic foraminiferal taxa (n = 27; ≥3% in at least one sample) using the results from all sites. PCA axes 1 and 2, respectively, explain 47% and 20% of the variance.

as this species prefers warmer waters (Caralp, 1989; Kaiho, 1994; McKay et al., 2015, 2016; Tetard et al., 2021a). The abundance of *B. marginata* and *P. neocarinata*, two other warmer-water species (Murray, 1991; Sen Gupta & Aharon, 1994; Platon, 2001), also increases towards the top of the sequence before disappearing between the late 1990s and the early 2000s at station 16, while the abundance of the colder-water species *N. labradorica*, *P. osloensis*, *E. clavatum*, and *V. arctica* (Vilks, 1969; Schafer & Cole, 1986; Knudsen et al., 1996; Polyak et al., 2002; Rytter et al., 2002) decreases (Fig. 5D). The increase in warmer-water species at the expense of colder-water species, paired with the disappearance of *N. labradorica*, a species associated with the LCW (Bilodeau et al., 1994), in the early 1960s in the GSL reflects changes in the relative contribution of parental waters to the LC observed in recent decades, more specifically a lower contribution of the LCW relative to the NACW (Gilbert et al., 2005; Jutras et al., 2020a, 2022).

PERSPECTIVE ON HISTORICAL AND LONGER TIME SCALES

From a recent historical perspective, the work of Hooper (1975) and Rodrigues & Hooper (1982) is interesting as it documents the distribution of benthic foraminifera in the LC in grab samples collected in the 1960s. Hence, a comparison between their data and ours allows for a further assessment of the evolution of the benthic environment over several decades. The most notable difference between our results and those of Hooper (1975) is the absence of *B. subaenariensis* in the LSLE and the overall higher taxonomic diversity. At the time of sampling by Hooper (1975) in 1965,

bottom-water DO concentrations at the western edge of the GSL were likely in excess of ~95 µM (see Fig. 6).

In the assemblages from the GSL that were described by Rodrigues & Hooper (1982), the dominance of *E. clavatum* and *S. concava* (as *Fursenkoina loeblichi*; Rodrigues & Hooper, 1982) is a contrasting feature from what we observe in our cores, and in the GSL in general (Genovesi et al., 2011). *Elphidium clavatum* is an opportunistic species typically associated with low organic carbon fluxes, low salinity, and relatively cold and well-oxygenated waters (Knudsen et al., 1996; Sen Gupta, 1999; Karlsen et al., 2000), although some studies report its occurrence in oxygen-depleted waters (e.g., Sen Gupta et al., 1996). Likewise, *Stainforthia* has been described as an opportunistic genus associated with high seasonal productivity and cold waters (Alve, 1995; Gustafsson & Nordberg, 2001; Polyak et al., 2002), and *S. concava* has been associated with Arctic waters (Lloyd et al., 2007). Thus, changes from assemblages dominated by *E. clavatum* and *S. concava* to assemblages dominated by *E. exilis*, as those we observe in zone 1 of all our study cores, could result from the change in the relative contribution of the parental waters and/or the concomitant warming of the bottom waters, both of which impact the benthic ecology, including oxygenation on the sea floor. It is difficult to disentangle these interrelated parameters. Nevertheless, our data and RDA results imply that the DO content is ultimately the primary parameter affecting the foraminiferal assemblages.

In order to go beyond the qualitative considerations about DO, we used our data set to develop a tool to reconstruct changes in bottom-water oxygenation. To do so, we considered the PC1 score of foraminiferal assemblages from
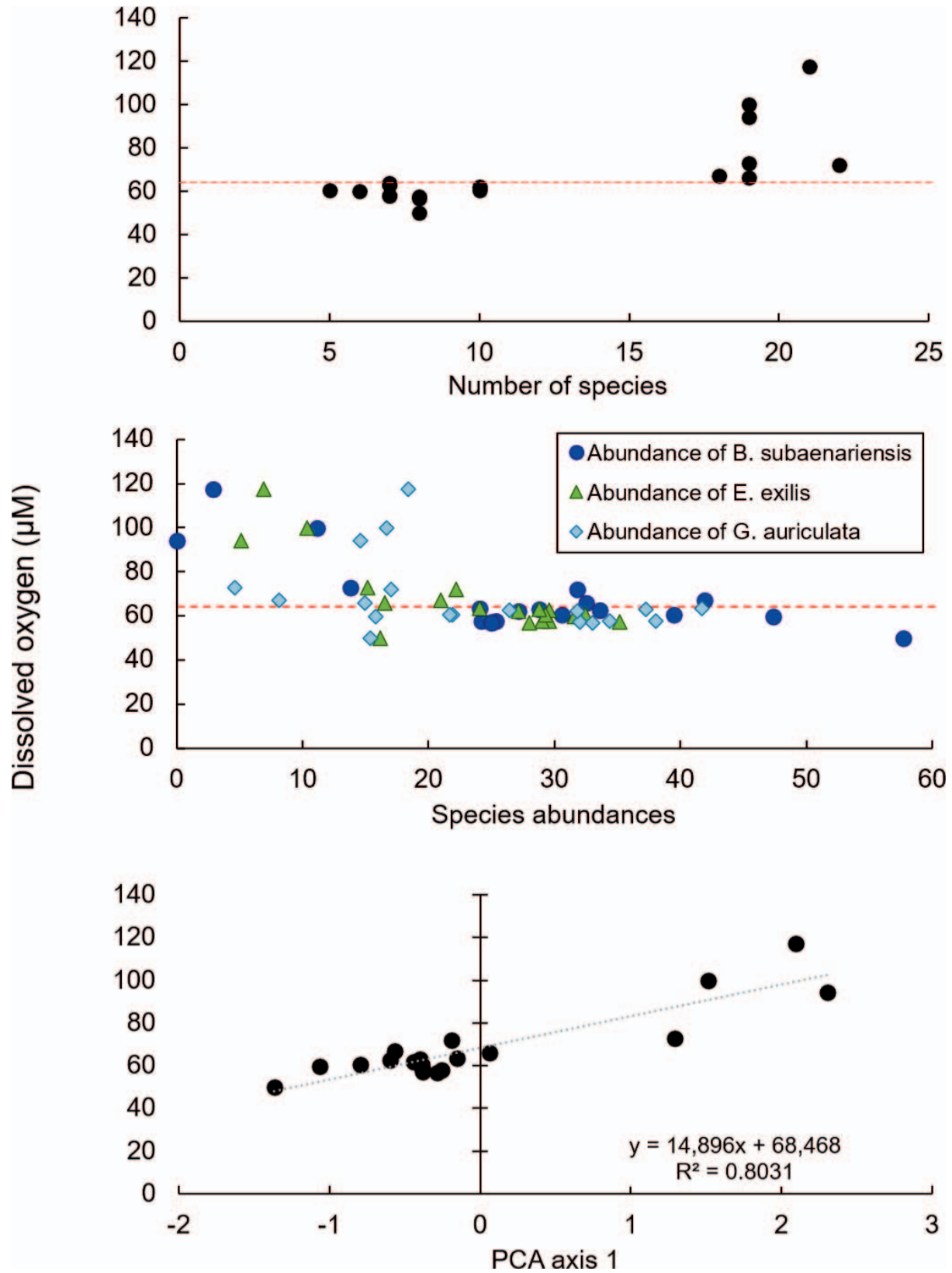
FIGURE 8. Relation between dissolved oxygen (DO) concentrations (µM), number of calcareous benthic foraminifera species, abundance of the three most dominant taxa, and PCA axis 1 score of foraminiferal assemblages at station 23 in the LSLE. PCA axis 1 explains 61% of the variance. The dotted line indicates the severe hypoxia threshold (<62.5 µM). The regression could be used as a regional transfer function to reconstruct DO concentrations with an error (1σ) of ±7.5 µM.
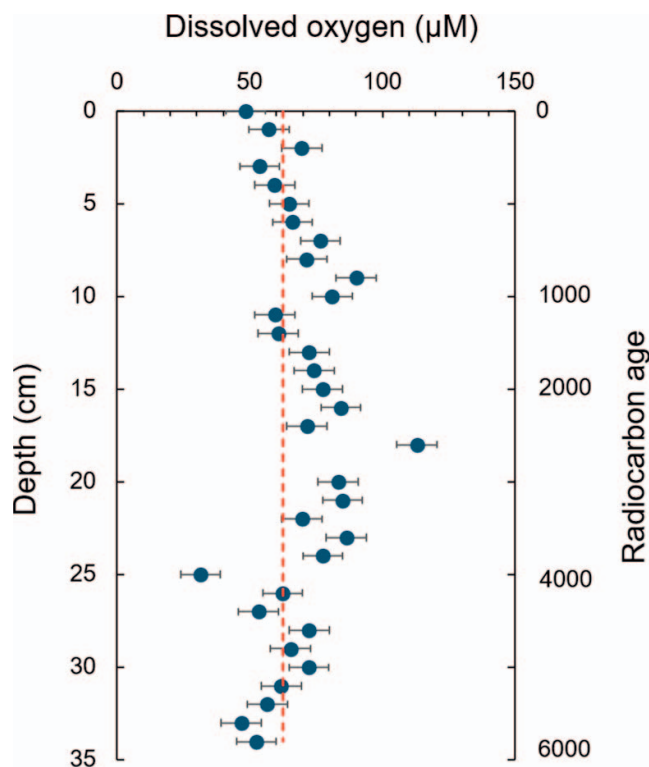
FIGURE 9. Tentative reconstruction of dissolved oxygen (DO; µM) concentrations over the past 6,000 years in the Esquiman Channel applying the regression of Fig. 8 on the dataset of Thibodeau et al. (2013; core CR06-TCE in Fig. 1). The dotted line corresponds to the severe hypoxia threshold (<62.5 µM), the error bar (±7.5 µM) corresponds to 1σ.

station 23. We believe that the high coefficient of correlation between PC1 and the DO concentration ($R^2 = 0.8031$; Fig. 8) justifies the elaboration of the following empirical equation:

$$[DO] = 14.896 \times PC1 + 68.468$$

As for the environmental interpretation of the three main groups described in the previous section, it should be noted that this relationship is specific to the LC in the LSLE. It might tentatively be applied in the GSL, but not in the global ocean. We thus tentatively applied the relationship to a long-time series from the Esquiman Channel in the eastern GSL (Core CR06-TCE, Fig. 1) to reconstruct the low oxygen event reported to have occurred between 4,000 and 6,000 years ago by Thibodeau et al. (2013). The tentative DO reconstruction presented in Figure 9 highlights hypoxic levels between 4,000 and 6,000 years ago.

CONCLUSION

The micropaleontological analyses we conducted on four sediment cores from the LC document the multidecadal succession of benthic foraminiferal assemblages and their rapid spatial and temporal evolution in response to changes in benthic environmental conditions in recent decades. The overall foraminiferal assemblages that include both cold- and warm-water species are complex. They likely relate to

variations in the contribution of both oxygen-rich polar water from the LWC and oxygen-poor warm water from the NACW.

Whereas the four study sites record a decrease in taxonomic diversity of ~60–65% across the LC since the 1960s, important changes in benthic foraminiferal assemblages are observed at approximately the same time at all studied sites, around the late 1990s and the early 2000s, coincident with the areal expansion of the hypoxic zone. We observe the decrease or disappearance of most taxa in favor of hypoxia-tolerant indicator species *Brizalina subaenariensis*, *Eubuliminella exilis*, and *Globobulimina auriculata*. These changes reflect how fast benthic foraminiferal assemblages respond to variations of bottom-water DO concentrations across the LC.

Whereas other environmental parameters such as temperature could explain multidecadal changes in the benthic microfauna, DO concentrations stand out as the major determinant parameter. Multivariate analyses highlight a close relationship between the benthic foraminiferal assemblages and bottom-water oxygen concentrations in the LSLE, from which we derived a regional proxy that allows us to estimate changes in bottom-water oxygenation prior to the period of instrumental measurements. This proxy deserves further calibration but appears promising to reconstruct the evolution of bottom-water oxygenation in relationship with large-scale changes in ocean circulation and their impact on the LSLE and the GSL during the present interglacial.

REFERENCES

Alve, E., 1995, Benthic foraminiferal distribution and recolonization of formerly anoxic environments in Drammensfjord, southern Norway: Marine Micropaleontology, v. 25, p. 169–186, DOI: 10.1016/0377-8398(95)00007-N.

Aquino-López, M. A., Blaauw, M., Christen, J. A., and Sanderson, N. K., 2018, Bayesian Analysis of [210]Pb Dating: Journal of Agricultural, Biological and Environmental Statistics, v. 23, p. 317–333, DOI: 10.1007/s13253-018-0328-7.

Belley, R., Archambault. P., Sundby, B., Gilbert, F., and Gagnon, J.-M., 2010, Effects of hypoxia on benthic macrofauna and bioturbation in the Estuary and Gulf of St. Lawrence, Canada: Continental Shelf Research, v. 30, p. 1302–1313.

Benoit, P., Gratton, Y., and Mucci, A., 2006, Modeling of dissolved oxygen levels in the bottom waters of the Lower St. Lawrence Estuary: Coupling of benthic and pelagic processes: Marine Chemistry, v. 102, p. 13–32.

Bernhard, J. M., 1988, Postmortem vital staining in benthic foraminifera; duration and importance in population and distributional studies: Journal of Foraminiferal Research, v. 18, p. 143–146, DOI: 10.2113/gsjfr.18.2.143.

Bernhard, J. M., Sen Gupta, B. K., and Borne, P. F., 1997, Benthic foraminiferal proxy to estimate dysoxic bottom-water oxygen concentrations; Santa Barbara Basin, U.S. Pacific continental margin: Journal of Foraminiferal Research, v. 27, p. 301–310, DOI: 10.2113/gsjfr.27.4.301.

Bilodeau, G., de Vernal, A., and Hillaire-Marcel, C., 1994, Benthic foraminiferal assemblages in Labrador Sea sediments: Relations with deep-water mass changes since deglaciation: Canadian Journal of Earth Sciences, v. 31, p. 128–138, DOI: 10.1139/e94-011.

Bourgault, D., and Koutitonsky, V. G., 1999, Real-time monitoring of the freshwater discharge at the head of the St. Lawrence Estuary: Atmosphere-Ocean, v. 37, p. 203–220.

Breitburg, D., 2002, Effects of hypoxia, and the balance between hypoxia and enrichment, on coastal fishes and fisheries: Estuaries, v. 25, p. 767–781, DOI: doi.org/10.1007/BF02804904

Brüchert, V., Pérez, M. E., and Lange, C. B., 2000, Coupled primary production, benthic foraminiferal assemblage, and sulfur diagenesis in organic-rich sediments of the Benguela upwelling system: Marine Geology, v. 163, p. 27–40, DOI: 10.1016/S0025-3227(99)00099-7.

Bugden, G. L., 1991, Changes in the temperature-salinity characteristics of the deeper waters of the Gulf of St. Lawrence over the past several decades, in Therriault, J.-C., (ed.), The Gulf of St. Lawrence: Small ocean or big estuary?: Canadian Special Publication of Fisheries and Aquatic Sciences, Canada, v. 113, p. 139–147.

Cage, A. G., Pieńkowski, A. J., Jennings, A., Knudsen, K. L., and Seidenkrantz, M.-S., 2021, Comparative analysis of six common foraminiferal species of the genera Cassidulina, Paracassidulina and Islandiella from the Arctic-North Atlantic domain: Journal of Micropalaeontology, v. 40, p. 37–60, DOI: 10.5194/jm-40-37-2021.

Caralp, M. H., 1989, Abundance of Bulimina exilis and Melonis barleeanum: Relationship to the quality of marine organic matter: Geo-Marine Letters, v. 9, p. 37–43, DOI: 10.1007/BF02262816.

Chabot, D., and Dutil, J. D., 1999, Reduced growth of Atlantic cod in non-lethal hypoxic conditions: Journal of Fish Biology, v. 55, p. 472–491, DOI: 10.1111/j.1095-8649.1999.tb00693.x.

Coplen, T. B., 1995, Discontinuance of SMOW and PDB: Nature, 375, p. 285, DOI : 10.1038/375285a0.

Corliss, B. H., and Emerson, S., 1990, Distribution of Rose Bengal stained deep-sea benthic foraminifera from the Nova Scotian continental margin and Gulf of Maine: Deep Sea Research Part A, Oceanographic Research Papers, v. 37, p. 381–400. DOI: 10.1016/0198-0149(90)90015-N.

Cushman, J. A., 1922, The Foraminifera of the Atlantic Ocean: United States National Museum Bulletin, No. 104, pt. 3, p. 1–149.

D'Amours, D., 1993, The distribution of cod (Qadus morhua) in relation to temperature and oxygen level in the Gulf of St. Lawrence: Fisheries Oceanography, v. 2, p. 24–29, DOI: 10.1111/j.1365-2419.1993.tb00009.x

de Vernal, A., Henry, M., and Bilodeau, G., 1999, Techniques de préparation et d'analyse en micropaléontologie: Les Cahiers du GEOTOP, Montreal, 28 p.

Dickie, L., and Trites, R., 1983, The Gulf of St. Lawrence, in Ketchum, B. (ed.), Ecosystems of the World: Estuaries and enclosed seas: NY: Elsevier, New York, p. 403–425.

Dinauer, A., and Mucci A., 2018, Distinguishing between physical and biological controls on the spatial variability of pCO_2: A novel approach using OMP water mass analysis

(St. Lawrence, Canada): Marine Chemistry, v. 204, p. 107–120, DOI: 10.1016/j.marchem.2018.03.007.

Dupont-Prinet, A., Pillet, M., Chabot, D., Hansen, T., Tremblay, R., and Audet, C., 2013, Northern shrimp (Pandalus borealis) oxygen consumption and metabolic enzyme activities are severely constrained by hypoxia in the Estuary and Gulf of St. Lawrence: Journal of Experimental Marine Biology and Ecology, v. 448, p. 298–307, DOI: 10.1016/j.jembe.2013.07.019.

Edenborn, H. M., Silverberg, N., Mucci, A., and Sundby, B., 1987, Sulfate reduction in deep coastal marine sediments: Marine Chemistry, v. 21, p. 329–345, DOI: 10.1016/0304-4203(87)90055-7.

Erdem, Z., Schönfeld, J., Rathburn, A. E., Pérez, M.-E., Cardich, J., and Glock, N., 2020, Bottom-water deoxygenation at the Peruvian margin during the last deglaciation recorded by benthic foraminifera: Biogeosciences, v. 17, p. 3165–3182. DOI: 10.5194/bg-17-3165-2020.

Fisheries and Oceans Canada (DFO), 2019, BioChem: Database of biological and chemical oceanographic data, Retrieved from http://www.dfo-mpo.gc.ca/science/data-donnees/biochem/index-eng.html.

Flynn, W., 1968, The determination of low levels of polonium-210 in environmental materials: Analytica Chimica Acta, v. 43, p. 221–227.

Fontanier, C., Jorissen, F. J., Licari, L., Alexandre, A., Anschutz, P., and Carbonel, P., 2002, Live benthic foraminiferal faunas from the Bay of Biscay: Faunal density, composition, and microhabitats: Deep-Sea Research I, v. 49, p. 751–785.

Galbraith, P. S., 2006, Winter water masses in the Gulf of St. Lawrence: Journal of Geophysical Research: Oceans, v. 111, DOI: 10.1029/2005JC003159.

Genovesi, L., de Vernal, A., Thibodeau, B., Hillaire-Marcel, C., Mucci, A., and Gilbert, D., 2011, Recent changes in bottom water oxygenation and temperature in the Gulf of St. Lawrence: Micropaleontological and geochemical evidence: Limnology and Oceanography, v. 56, p. 1319–1329.

Gilbert, D., 2004, Propagation of temperature signals along the northwest Atlantic continental shelf edge and into the Laurentian Channel, in Abstract, ICES CIEM Annual Science Conference September, p. 22–25.

Gilbert, D., and Pettigrew, B., 1997, Interannual variability (1948–1994) of the CIL core temperature in the Gulf of St. Lawrence: Canadian Journal of Fisheries and Aquatic Sciences, v. 54, p. 57–67.

Gilbert, D., Sundby, B., Gobeil, C., Mucci, A., and Tremblay, G. H., 2005, A seventy-two-year record of diminishing deep-water oxygen in the St. Lawrence estuary: The northwest Atlantic connection: Limnology and Oceanography, v. 50, p. 1654–1666.

Gustafsson, M., and Nordberg, K., 2001, Living (stained) benthic foraminiferal response to primary production and hydrography in the deepest part of the Gullmar Fjord, Swedish West Coast, with comparisons to Hoglund's 1927 material: Journal of Foraminiferal Research, v. 31, p. 2–11, DOI: 10.2113/0310002.

Hoogakker, B. A. A., Lu, Z., Umling, N., Jones, L., Zhou, X., Rickaby, R. E. M., Thunell, R., Cartapanis, O., and Galbraith, E., 2018, Glacial expansion of oxygen-depleted seawater in the eastern tropical Pacific: Nature, v. 562, p. 410–413, DOI: 10.1038/s41586-018-0589-x.

Hooper, K., 1975, Foraminiferal ecology and associated sediments of the lower St. Lawrence Estuary: Journal of Foraminiferal Research, v. 5, p. 218–238, DOI: 10.2113/gsjfr.5.3.218.

Jennings, A., Andrews, J. T., Reilly, B., Walczak, M., Jakobsson, M., Mix, A., Stoner, J., Nicholls, K.W., and Cheseby, M., 2020, Modern foraminiferal assemblages in northern Nares Strait, Petermann Fjord, and beneath Petermann Ice Tongue, NW Greenland: Arctic, Antarctic, and Alpine Research, v. 52, p. 491–511.

Jorissen, F. J., Fontanier, C., and Thomas, E., 2007, Paleoceanographical proxies based on deep-sea benthic foraminiferal assemblage characteristics: Developments in Marine Geology, v. 1, p. 263–325.

Jutras, M., Dufour, C. O., Mucci, A., Cyr, F., and Gilbert, D., 2020a, Temporal changes in the causes of the observed oxygen decline in the St. Lawrence Estuary: Journal of Geophysical Research: Oceans, v. 125, DOI: 10.1029/2020JC016577.

Jutras, M., Mucci, A., Sundby, B., Gratton, Y., and Katsev, S., 2020b, Nutrient cycling in the Lower St. Lawrence Estuary: Response to

environmental perturbations: Estuarine, Coastal and Shelf Science, v. 239, DOI: 10.1016/j.ecss.2020.106715.

Jutras, M., Mucci, A., Chaillou, G., Nesbitt, W. A., and Wallace, D. W. R., 2022, Temporal and spatial evolution of bottom-water hypoxia in the Estuary and Gulf of St. Lawrence: EGUsphere [preprint], DOI: 10.5194/egusphere-2022-1090.

Kaiho, K., 1994, Benthic foraminiferal dissolved-oxygen index and dissolved-oxygen levels in the modern ocean: Geology, v. 22, p. 719–722, DOI: 10.1130/0091-7613(1994)022<0719:Bfdoia>2.3.Co;2.

Karlsen, A. W., Cronin, T. M., Ishman, S. E., Willard, D. A., Kerhin, R., Holmes, C. W., and Marot, M., 2000, Historical trends in Chesapeake Bay dissolved oxygen based on benthic foraminifera from sediment cores: Estuaries, v. 23, p. 488–508, DOI: 10.2307/1353141.

Knudsen, K. L., Conradsen, K., Heier-Nielsen, S., and Seidenkrantz, M.-S., 1996, Palaeoenvironments in the Skagerrak-Kattegat basin in the eastern North Sea during the last deglaciation: Boreas, v. 25, p. 65–78, DOI: 10.1111/j.1502-3885.1996.tb00836.x.

Lloyd, J. M., Kuijpers, A., Long, A., Moros, M., and Park, L. A., 2007, Foraminiferal reconstruction of mid- to late-Holocene Ocean circulation and climate variability in Disko Bugt, West Greenland: The Holocene, v. 17, p. 1079–1091, DOI: 10.1177/0959683607082548.

Loeblich, A. R. and Tappan, H., 1987, Foraminiferal Genera and Their Classification: Van Nostrand Reinhold Company, New York, 970 p.

McKay, C. L., Groeneveld, J., Filipsson, H. L., Gallego-Torres, D., Whitehouse, M. J., Toyofuku, T., and Romero, O. E., 2015, A comparison of benthic foraminiferal Mn/Ca and sedimentary Mn/Al as proxies of relative bottom-water oxygenation in the low-latitude NE Atlantic upwelling system: Biogeosciences, v. 12, p. 5415–5428, DOI: 10.5194/bg-12-5415-2015.

McKay, C. L., Filipsson, H. L., Romero, O. E., Stuut, J.-B. W., and Björck, S., 2016, The interplay between the surface and bottom water environment within the Benguela Upwelling System over the last 70 ka: Paleoceanography, v. 31, p. 266–285, DOI: 10.1002/2015PA002792.

Meyers, P. A., 1997, Organic geochemical proxies of paleoceanographic, paleolimnologic, and paleoclimatic processes: Organic Geochemistry, v. 27, p. 213–250, DOI: 10.1016/S0146-6380(97)00049-1.

Murray, J. W., 1991, Ecology and Paleoecology of Benthic Foraminifera: Longman Scientific and Technical, London, 397 p.

Muzuka, A. N., and Hillaire-Marcel, C., 1999, Burial rates of organic matter along the eastern Canadian margin and stable isotope constraints on its origin and diagenetic evolution: Marine Geology, v. 160, p. 251–270, DOI: 10.1016/S0025-3227(99)00022-5.

Ohkushi, K., Kennett, J. P., Zeleski, C. M., Moffitt, S. E., Hill, T. M., Robert, C., Beaufort, L., and Behl, R. J., 2013, Quantified intermediate water oxygenation history of the NE Pacific: A new benthic foraminiferal record from Santa Barbara basin: Paleoceanography, v. 28, p. 453–467.

Osterman, L. E., 2003, Benthic foraminifers from the continental shelf and slope of the Gulf of Mexico: An indicator of shelf hypoxia: Estuarine, Coastal and Shelf Science, v. 58, p. 17–35, DOI: 10.1016/S0272-7714(02)00352-9.

Osterman, L. E., Poore, R. Z., and Foley, K. M., 1999, Distribution of benthic foraminifers (>125 μm) in the surface sediments of the Arctic Ocean: U.S. Geological Survey Bulletin, v. 2164, p. 1–28.

Overpeck, J. T., Webb, T. I. I. I., and Prentice, I. C., 1985, Quantitative interpretation of fossil pollen spectra: Dissimilarity coefficients and the method of modern analogs: Quaternary Research, v. 23, p. 87–108, DOI: 10.1016/0033-5894(85)90074-2.

Ovsepyan, E., Ivanova, E., Tetard, M., Max, L., and Tiedemann, R., 2021, Intermediate-and deep-water oxygenation history in the subarctic North Pacific during the last deglacial period: Frontiers in Earth Science, v. 9, DOI: 10.3389/feart.2021.638069.

Parker, F. L., 1954, Distribution of the foraminifera in the northwest Gulf of Mexico: Bulletin of the Museum of Comparative Zoology, v. 111, p. 453–588.

Phleger, F. B., and Parker, F. L., 1951, Ecology of Foraminifera, Northwest Gulf of Mexico, Part II. Foraminifera Species: The Geological Society of America, Memoir, v. 46, p. 1–64.

Platon, E., 2001, Benthic Foraminifera in Two Stressed Environments of the Northern Gulf of Mexico: LSU Historical Dissertations and Theses, v. 307, 291 p., Retrieved from https://digitalcommons.lsu.edu/gradschool_disstheses/307.

Platon, E., Gupta, B. K. S., Rabalais, N. N., and Turner, R. E., 2005, Effect of seasonal hypoxia on the benthic foraminiferal community of the Louisiana inner continental shelf: The 20th century record: Marine Micropaleontology, v. 54, p. 263–283, DOI: 10.1016/j.marmicro.2004.12.004.

Polyak, L., Korsun, S., Febo, L. A., Stanovoy, V., Khusid, T., Hald, M., Paulsen, B. E., and Lubinski, D.J., 2002, Benthic foraminiferal assemblages from the southern Kara Sea, a river-influenced Arctic marine environment: Journal of Foraminiferal Research, v. 32, p. 252–273, DOI: 10.2113/32.3.252.

R Core Team, 2021, R: A language and environment for statistical computing: R Foundation for Statistical Computing, Vienna, Austria.

Rasmussen, T. L., and Thomsen, E., 2004, The role of the North Atlantic Drift in the millennial timescale glacial climate fluctuations: Palaeogeography, Palaeoclimatology, Palaeoecology, v. 210, p. 101–116, DOI: 10.1016/j.palaeo.2004.04.005.

Rodrigues, C. G.,1980, Holocene microfauna and paleoceanography of the Gulf of St. Lawrence, Ph.D. Thesis, Carleton University, 352 p.

Rodrigues, C. G., and Hooper, K., 1982, Recent benthonic foraminiferal associations from offshore environments in the Gulf of St. Lawrence: Journal of Foraminiferal Research, v. 12, 327–352, DOI: 10.2113/gsjfr.12.4.327.

Rytter, F., Knudsen, K. L., Seidenkrantz, M.-S., and Eiríksson, J., 2002, Modern distribution of benthic foraminifera on the North Icelandic shelf and slope: Journal of Foraminiferal Research, v. 32, p. 217–244, DOI: 10.2113/32.3.217.

Saucier, F., Roy, F., Senneville, S., Smith, G., Lefaivre, D., Zakardjian, B., and Dumais, J., 2009, Modelling of the circulation in the estuary and the Gulf of St. Lawrence in response to variations in fresh water runoff and winds: Journal of Water Science, v. 22, p. 159–176.

Schafer, C. T., and Cole, F. E., 1986, Reconnaissance survey of benthonic foraminifera from Baffin Island Fjord environments: Arctic, v. 39, p. 232–239.

Sen Gupta, B. K., 1999, Modern Foraminifera: Kluwer Academic Publishers, Dordrecht, 371 p.

Sen Gupta, B. K., and Aharon, P., 1994, Benthic foraminifera of bathyal hydrocarbon vents of the Gulf of Mexico: Initial report on communities and stable isotopes: Geo-Marine Letters, v. 14, p. 88–96, DOI: 10.1007/BF01203719.

Sen Gupta, B. K., and Machain-Castillo, M. L., 1993, Benthic foraminifera in oxygen-poor habitats: Marine Micropaleontology, v. 20, p. 183–201, DOI: 10.1016/0377-8398(93)90032-S.

Sen Gupta, B. K., Eugene Turner, R., and Rabalais, N. N., 1996, Seasonal oxygen depletion in continental-shelf waters of Louisiana: Historical record of benthic foraminifers: Geology, v. 24, p. 227–230, DOI: 10.1130/0091-7613(1996)024<0227:Sodics>2.3.Co;2.

Smith, G., Saucier, F., and Straub, D., 2006, Formation and circulation of the cold intermediate layer in the Gulf of Saint Lawrence: Journal of Geophysical Research, Oceans, v. 111, DOI: 10.1029/2005JC003017.

ter Braak, C. J., and Smilauer, P., 2012, Canoco reference manual and user's guide: Software for ordination, version 5.0.

Tetard, M., Beaufort, L., and Licari, L., 2017, A new optical method for automated pore analysis on benthic foraminifera: Marine Micropaleontology, v. 136, p. 30–36.

Tetard, M., Ovsepyan, E., and Licari, L., 2021a, *Eubuliminella tenuata* as a new proxy for quantifying past bottom water oxygenation: Marine Micropaleontology, v. 166, DOI: 10.1016/j.marmicro.2021.102016.

Tetard, M., Licari, L., Ovsepyan, E., Tachikawa, K., and Beaufort, L., 2021b, Toward a global calibration for quantifying past oxygenation in oxygen minimum zones using benthic Foraminifera: Biogeosciences, v. 18, p. 2827–2841, DOI: 10.5194/bg-18-2827-2021.

Thibodeau, B., de Vernal, A., and Mucci, A., 2006, Recent eutrophication and consequent hypoxia in the bottom waters of the Lower St. Lawrence Estuary: Micropaleontological and geochemical evidence: Marine Geology, v. 231, p. 37–50.

Thibodeau, B., Lehmann, M. F., Kowarzyk, J., Mucci, A., Gélinas, Y., Gilbert, D., Maranger, R., and Alkhatib, M., 2010, Benthic

nutrient fluxes along the Laurentian Channel: Impacts on the N budget of the St. Lawrence marine system: Estuarine, Coastal and Shelf Science, v. 90, p. 195–205, DOI: 10.1016/j.ecss.2010.08.015.

Thibodeau, B., de Vernal, A., and Limoges, A., 2013, Low oxygen events in the Laurentian Channel during the Holocene, Marine Geology, v. 346, p. 183–191, DOI: 10.1016/j.margeo.2013.08.004.

Thibodeau, B., Not, C., Zhu, J., Schmittner, A., Noone, D., Tabor, C., Zhang, J., and Liu, Z., 2018, Last century warming over the Canadian Atlantic shelves linked to weak Atlantic meridional overturning circulation: Geophysical Research Letters, v. 45, p. 12,376–12,385, DOI: 10.1029/2018GL080083.

Tichenor, H. R., 2013, Foraminifera as indicators of hypoxia off Southwest Pass, Mississippi Delta, Gulf of Mexico?: MSc Thesis, East Carolina University, Greenville, 70 p.

Vilks, G., 1969, Recent Foraminifera in the Canadian Arctic: Micropaleontology, v. 15, p. 35–60, DOI: 10.2307/1484859.

Vilks, G., and Rashid, M. A., 1976, Post-glacial paleo-oceanography of Emerald Basin, Scotian Shelf: Canadian Journal of Earth Sciences, v. 13, p. 1256–1267.

APPENDIX

TABLE A1. List and taxonomic remarks for all calcareous benthic foraminiferal taxa in sediments of the LC of the LSLE and GSL. The taxa are listed separately in alphabetical order of class and family. However, several taxa are grouped in the figures and statistical data treatment in this study; these groups are identified under remarks. Common taxa make up >10% of the assemblages. Occasional taxa make up between 3 and 10% of the assemblages. Rare taxa make up <3% of the assemblages.

Family	Genus	Species	Author	Relative abundance	Remarks
ALABAMINIDAE	*Oridorsalis*	*tener*	Brady, 1884	Rare LSLE – GSL	
ASTRONONIONIDAE	*Astrononion*	*gallowayi*	Loeblich & Tappan, 1953	Rare LSLE – GSL	
BOLIVINITIDAE	*Bolivina*	cf. *alata.*	Seguenza, 1862	Rare LSLE – GSL	Unknown species tentatively ascribed to *B. alata*
	Bolivinellina	*pseudopunctata*	Höglund, 1947	Occasional LSLE – GSL	
	Sagrina	*subspinescens*	Cushman, 1922	Occasional LSLE – Rare GSL	
	Brizalina	*subaenariensis*	Cushman, 1922	Common LSLE – GSL	
BULIMINIDAE	*Bulimina*	*marginata*	d'Orbigny, 1826	Common LSLE – GSL	May have been identified as *Bulimina aculeata* in Hooper (1975) and Rodrigues & Hooper (1982)
CANCRISIDAE	*Valvulineria*	*arctica*	Green, 1959	Rare LSLE – Occasional GSL	
CASSIDULINIDAE	*Cassidulina*	*laevigata*	d'Orbigny, 1826	Rare LSLE – Occasional GSL	*C. laevigata* and *C. neoteretis* are grouped in the data treatment in this study, as there are only very few and indistinctive *C. laevigata*
		neoteretis	Seidenkrantz, 1995	Rare LSLE – Occasional GSL	
		reniforme	Nørvang, 1945	Occasional LSLE – GSL	
		obtusa	Williamson, 1858	Rare LSLE – GSL	
	Islandiella	*helenae*	Feyling-Hanssen & Buzas, 1976	Rare LSLE – Absent GSL	
		islandica	Nørvang, 1945	Occasional LSLE – Rare GSL	Referred to as *Cassidulina islandica* in Hooper (1975)
		norcrossi	Cushman, 1933	Occasional LSLE – Rare GSL	
	Paracassidulina	*neocarinata*	Thalmann, 1950	Rare LSLE – Occasional GSL	
CIBICIDIDAE	*Cibicidoides*	*pachydermus*	Rzehak, 1886	Rare LSLE – GSL	All species of *Cibicidoides* are grouped in the data treatment of this study
		wuellerstorfi	Schwager, 1866	Rare LSLE – Occasional GSL	
		sp.		Absent LSLE – Rare GSL	
ELPHIDIIDAE	*Elphidium*	*clavatum*	Cushman, 1930	Common LSLE – GSL	These species are grouped as *Elphidium* spp. in this study
		selseyense	Heron-Allen & Earland, 1911	Rare LSLE – GSL	
EPONIDIDAE	*Alabaminella*	*weddellensis*	Earland, 1936	Rare LSLE – Occasional GSL	
GAVELINELLIDAE	*Gyroidina*	*lamarckiana*	d'Orbigny, 1839	Occasional LSLE – GSL	
GLOBOBULIMINIDAE	*Globobulimina*	*auriculata*	Bailey, 1894	Common LSLE – GSL	
		turgida	Bailey, 1851	Absent LSLE – Rare GSL	
NONIONIDAE	*Nonionellina*	*labradorica*	Dawson, 1860	Common LSLE – GSL	
	Nonionoides	*turgidus*	Williamson, 1858	Rare LSLE – GSL	
PULLENIIDAE	*Pullenia*	*osloensis*	Feyling-Hanssen, 1954	Common LSLE – GSL	
STAINFORTHIIDAE	*Stainforthia*	*concava*	Höglund, 1947	Occasional LSLE – GSL	May have been identified as *Fursenkoina loeblichi* in Rodrigues & Hooper (1982)
		fusiformis	Williamson, 1858	Rare LSLE – GSL	
TRICHOHYALIDAE	*Buccella*	*frigida*	Cushman, 1922	Rare LSLE – Occasional GSL	
	Buccella	sp.		Rare LSLE – GSL	
TURRILINIDAE	*Eubuliminella*	*exilis*	Brady, 1884	Common LSLE – GSL	
ELLIPSOLAGENIDAE	*Cushmanina*	*quadralata*	Brady, 1881	Absent LSLE – Rare GSL	Species of *Cushmanina* are grouped under the name "*Lagena/Oolina* spp." in the figures and data treatment of this study
	Fissurina	spp.	Reuss, 1850	Rare LSLE – Occasional GSL	*Fissurina/ Parafissurina* are grouped together in the data treatment of this study

TABLE A1. Continued

Family	Genus	Species	Author	Relative abundance	Remarks
	Oolina	*borealis*	Loeblich & Tappan, 1954	Absent LSLE – Rare GSL	Species of *Oolina* are grouped under the name "*Lagena/Oolina* spp." in the figures and data treatment of this study
GLANDULINIDAE	*Glandulina*	*hexagona*	Williamson, 1848		
		laevigata	d'Orbigny, 1826	Rare LSLE – Occasional GSL	*G. laevigata* and Polymorphinidae are grouped together under the name "Polymorphinidae" in the data treatment of this study
	Parafissurina	spp.	Parr, 1947	Rare LSLE – Occasional GSL	*Fissurina/ Parafissurina* are grouped together in the data treatment of this study
HAUERINIDAE	*Quinqueloculina*	*seminulum*	Linnaeus, 1758	Rare LSLE – Occasional GSL	
	Triloculina	*trigonula*	Lamarck, 1804	Absent LSLE – Rare GSL	
		tricarinata	Deshayes, 1832	Absent LSLE – Rare GSL	
	Pyrgo	*williamsoni*	Silvestri, 1923	Rare LSLE – Occasional GSL	
	Miliolinella	*subrotunda*	Montagu, 1803	Absent LSLE – Occasional GSL	
LAGENIDAE	*Lagena*	*gracilis*	Williamson, 1848	Occasional LSLE – GSL	Species of the genera *Lagena* and *Reussoolina* are grouped under the name "*Lagena/Oolina* spp." in the figures and data treatment of this study
		hispidula	Cushman, 1913		
		mollis	Brady, 1881		
		nebulosa	Cushman, 1923		
		striata	d'Orbigny, 1839		
	Reussoolina	*laevis*	Montagu, 1803		
POLYMORPHINIDAE	*Guttulina*	spp.	d'Orbigny, 1839	Rare LSLE – Occasional GSL	Grouped under "*Polymorphinidae*" in this study
SPIROLOCULINIDAE	*Spiroloculina*	sp. A		Absent LSLE – Rare GSL	Only a single specimen was observed
VAGINULINIDAE	*Lenticulina*	*gibba*	d'Orbigny, 1839	Rare LSLE – GSL	

FIGURE A1. Keyence^TM microscope photographs of selected benthic foraminiferal species from the Laurentian Channel. All scale bars = 100 μm. **1** *Alabaminella weddellensis* (Earland, 1936) **2** *Bolivina* cf. *alata* (Seguenza, 1862) **3** *Bolivinellina pseudopunctata* (Höglund, 1947) **4** *Brizalina subaenariensis* (Cushman, 1922) **5a** *Buccella frigida* (Cushman, 1922) dorsal view **5b** *B. frigida* ventral view **6** *Bulimina marginata* (d'Orbigny, 1826) **7** *Cassidulina laevigata* (d'Orbigny, 1826) **8** *Cassidulina neoteretis* (Seidenkrantz, 1995) **9** *Cassidulina reniforme* (Nørvang, 1945) **10** *Cassidulina obtusa* (Williamson, 1858) **11a** *Cibicidoides pachydermus* (Rzehak, 1886) dorsal view **11b** *C. pachydermus* ventral view **12a** *Cibicidoides wuellerstorfi* (Schwager, 1866) dorsal view **12b** *C. wuellerstorfi* ventral view **13a, 13b** *Elphidium clavatum* (Cushman, 1930) **14** *Elphidium selseyense* (Heron-Allen & Earland, 1911) **15** *Eubuliminella exilis* (Brady, 1884) **16** *Glandulina laevigata* (d'Orbigny, 1826) **17** *Globobulimina auriculata* (Bailey, 1894)

FIGURE A2. Keyence[TM] microscope photographs of selected benthic foraminiferal species from the Laurentian Channel. All scale bars = 100 μm. **1** *Gyroidina lamarckiana* (d'Orbigny, 1839) **2** *Islandiella islandica* (Nørvang, 1945) **3** *Islandiella norcrossi* (Cushman, 1933) **4** *Lagena gracilis* (Williamson, 1848) **5** *Lagena mollis* (Brady, 1881) **6** *Cushmanina quadralata* (Brady, 1881) **7** *Lenticulina gibba* (d'Orbigny, 1839) **8** *Nonionellina labradorica* (Dawson, 1860) **9** *Nonionoides turgidus* (Williamson, 1858) **10** *Oolina borealis* (Loeblich & Tappan, 1954) **11a** *Oridorsalis tener* (Brady, 1884) dorsal view **11b** *O. tener* ventral view **12** *Paracassidulina neocarinata* (Thalmann, 1950) **13** *Fissurina* sp. (Reuss, 1850) **14** *Pullenia osloensis* (Feyling-Hanssen, 1954) **15** *Pyrgo williamsoni* (Silvestri, 1923) **16** *Quinqueloculina seminulum* (Linnaeus, 1758) **17** *Reussoolina laevis* (Montagu, 1803) **18** *Sagrina subspinescens* (Cushman, 1922) **19** *Stainforthia oncave* (Höglund, 1947) **20** *Triloculina tricarinata* (Deshayes, 1832) **21** *Valvulineria arctica* (Green, 1959)

SUPPLEMENTARY MATERIALS CAPTIONS

TABLE S1. RDA axes 1 and 2 scores of calcareous benthic foraminiferal taxa at station 23 with dissolved oxygen (DO), temperature, ratio of organic carbon to total nitrogen ($C_{org}:N_{tot}$), and $\delta^{13}C_{org}$, as environmental variables. RDA axes 1 and 2, respectively, explain 52% and 11% of the variance. Species with the highest and lowest scores in bold. The multivariate analyses were done using the CANOCO 5 software (Ter Braak & Šmilauer, 2012).

TABLE S2. Record of dissolved oxygen (DO) concentrations at 250 to 355 m of water depth in the LSLE based on data extracted in 2018 from the BioChem database made available by the Department of Fisheries and Oceans Canada, and a compilation of data acquired on the *R/V Coriolis II* (extended from Gilbert et al., 2005; Jutras et al., 2020a).

TABLE S3. A comparison of taxa identified by Hooper (1975), Rodrigues & Hooper (1982) and our study in the LC sediments. Large circles correspond to frequent occurrences, small circles to presence, whereas "x" indicate an absence in the sediments. If Hooper (1975), Rodrigues & Hooper (1982) used a different species name than the name used in this study, this former name is given in brackets below the name used by us.

TABLE S4. Raw counts of all foraminiferal taxa. Counts of fully and partially Rose Bengal-stained individuals are in parentheses besides the total number.

TABLE S5. Raw counts of individuals sized between 63 and 106 μm.

FIGURE S1. *Plum* age-depth models for **A** station 23 **B** station 21 **C** station 18.5 **D** station 16. The blue rectangles represent the ^{210}Pb activity (Bq kg^{-1}). The red line represents the mean model. The grey dashed lines are the 95% confidence intervals. The purple rectangles represent the ^{226}Ra activity (Bq kg^{-1}). The priors (green lines) and posteriors (grey plots) for each model are shown in the mini plots above the age-depth models. Based on estimated sedimentation rates, the prior parameters corresponding to accumulation rates (*acc.mean*) were set to 1.4 a cm^{-1}, 2 a cm^{-1}, 3 a cm^{-1}, and 10 a cm^{-1} for stations 23, 21, 18.5 and 16, respectively.

FIGURE S2. Ordination diagrams of calcareous benthic foraminiferal taxa (3% in at least one sample) from **A** Station 23 (n = 13). PCA axes 1 and 2, respectively, explain 61% and 30% of the variance. **B** Station 21 (n = 11). PCA axes 1 and 2, respectively, explain 60% and 20% of the variance. **C** Station 18.5 (n = 13). PCA axes 1 and 2, respectively, explain 81% and 7% of the variance. **D** Station 16 (n = 24). PCA axes 1 and 2, respectively explain 66% and 10% of the variance.

FIGURE S3. Ordination diagram of RDA of calcareous benthic foraminiferal taxa (n = 19; 3% of the calcareous assemblage in at least one sample), with dissolved oxygen (DO), temperature, ratio of organic carbon to total nitrogen ($C_{org}:N_{tot}$), and $\delta^{13}C_{org}$, as environmental variables at station 23 (see Table S1). RDA axes 1 and 2, respectively, explain 52% and 11% of the variance.